UNCLASSIFIED

CONFIDENTIAL

Copy No. 32

RM No. L8E11

NACA RM No. L8E11

Classification Changed to UNCLASSIFIED
NACA Res. Absth. #33, dated Dec. 3, 1952 (9-16-53)
Date 3-23-53 By J. E. Newman Jr.

NACA

JPL LIBRARY
CALIFORNIA INSTITUTE OF TECHNOLOGY

RESEARCH MEMORANDUM

PRELIMINARY INVESTIGATION TO DETERMINE PROPELLER SECTION CHARACTERISTICS BY MEASURING THE PRESSURE DISTRIBUTION ON AN NACA 10-(3)(08)-03 PROPELLER UNDER OPERATING CONDITIONS

By

Albert J. Evans and George Liner

Langley Aeronautical Laboratory
Langley Field, Va.

CASE FILE COPY

CLASSIFIED DOCUMENT

This document contains classified information affecting the National Defense of the United States within the meaning of the Espionage Act, USC 50:31 and 32. Its transmission or the revelation of its contents in any manner to an unauthorized person is prohibited by law. Information so classified may be imparted only to persons in the military and naval services of the United States, appropriate civilian officers and employees of the Federal Government who have a legitimate interest therein, and to United States citizens of known loyalty and discretion who of necessity must be informed thereof.

NATIONAL ADVISORY COMMITTEE FOR AERONAUTICS

WASHINGTON

July 14, 1948

CONFIDENTIAL

JUL 20 1948

UNCLASSIFIED

UNCLASSIFIED
Classification Changed to UNCLASSIFIED per NACA-Res Abstr. #33, dated Dec. 3, 1952 (9-16-53)
Date 3-23-53 By D. E. Kenlan per

NATIONAL ADVISORY COMMITTEE FOR AERONAUTICS

RESEARCH MEMORANDUM

PRELIMINARY INVESTIGATION TO DETERMINE PROPELLER SECTION CHARACTERISTICS BY MEASURING THE PRESSURE DISTRIBUTION ON AN NACA 10-(3)(08)-03 PROPELLER UNDER OPERATING CONDITIONS

By Albert J. Evans and George Liner

SUMMARY

An investigation has been made in the Langley 16-foot high-speed tunnel to determine the propeller-section characteristics by measuring the pressure distribution on the airfoil sections of a rotating propeller. The pressures were measured at nine radial stations on an NACA 10-(3)(08)-03 design two-blade propeller. This paper presents the results of the pressure measurements in the form of normal-force and moment coefficients and covers a range of nominal angle of attack (simple blade element theory) from 0° to 4° for a section Mach number range of approximately 0.6 to 1.15 for the outboard stations and approximately 0.3 to 0.6 for inboard stations.

INTRODUCTION

Since propeller sections operate at speeds considerably higher than the speeds encountered on other parts of an airplane, the propeller designer has continually been faced with a lack of airfoil data in the transonic speed range. Above the critical speed of the airfoil, nearly all data are subject to wind-tunnel choking effects, and extrapolation to high values of Mach number has proved of little value. Even if the two-dimensional data were available for supercritical values of Mach number, the effects of velocity gradient along the blade, the three-dimensional tip effects, and the action of centrifugal force on the boundary layer along the blade impose problems that need to be investigated on the operating propeller.

As a first step toward obtaining these data, tests have just been completed in the Langley 16-foot high-speed tunnel whereby section characteristics have been determined by measuring the pressure distribution on the rotating propeller-blade sections under operating conditions.

This paper presents a major portion of the data obtained from the tests and is of a preliminary nature. To expedite distribution no attempt has been made to analyze the data.

APPARATUS

Propeller dynamometer.- The tests were made on a 2000-horsepower propeller dynamometer in the Langley 16-foot high-speed tunnel. A complete description of the dynamometer is contained in reference 1.

Pressure-transfer device.- In the past there has existed no practical method of measuring the pressure distribution on a rotating propeller blade for more than one pressure orifice at a time, but recently a pressure-transfer device, using a mercury seal, has been developed at the Langley Laboratory of the National Advisory Committee for Aeronautics which allows 24 pressures to be measured simultaneously on a rotating airfoil. Pressure-transfer devices have been used heretofore by other investigators, but in most cases they have been single pressure-measuring devices or have incorporated too many inherent disadvantages to be of practical use.

A schematic view of two pressure cells in the transfer device is presented in figure 1. A detailed description is given in reference 2. The transfer device was mounted on the rear casing of the propeller dynamometer in such a way that there was no interference with the thrust- and torque-measuring mechanism. Flexible tubes connected the stationary outlet of the transfer device to a manometer board and the pressures were recorded by a remotely operated aerial camera.

Propeller blades.- The propeller blades are of solid dural construction and are designated the NACA 10-(3)(08)-03 design. These blades were chosen for the first tests because they incorporate the basic design of the NACA blades used in the investigation of propeller solidity, thickness, and camber. The digits in the propeller designation indicate a 10-foot-diameter propeller incorporating 16-series sections with the following design parameters at the 0.70-radius station, section design lift coefficient of 0.30, thickness of 8-percent chord, and a solidity of 0.03 per blade.

A complete description of the blades, together with the aerodynamic characteristics of the blades, is contained in reference 1. The blades were tested as a two-blade propeller for the present tests, and blade-form characteristic curves are presented in figure 2. Twelve radial grooves were cut in each surface of one of the blades at specified chordwise stations where it was desired to measure the pressure. The grooves were cut with a bottom radius and were close to the same size

UNCLASSIFIED

as the outside diameter of the tubes to be installed. The tubing was then laid in the grooves with the tops of the tubes flush with the surrounding surface of the blade and were retained in the blade by peening the edges of the grooves at intervals along the radius. A zinc metal spray was then applied, to fill in any cavities around the tubes, and allowed to harden. After hardening, the blade was carefully sanded to its original section shape. Orifices could then be drilled at any desired radial station. Nine stations were tested and were chosen so as to define clearly the thrust loading curve along the propeller blade.

The first pressure distributions were measured at the outboard station nearest the tip. When measurements at this station were complete, the orifices were plugged with a metallic plastic and a new set of holes drilled at the next desired inboard station.

In order to correct the pressures read on the manometer for the pressure due to the centrifugal force of the air column in a pressure tube, a resistance thermometer was installed in an additional groove cut into the lower surface or thrust face of the propeller blade at the 50-percent-chord station. The thermometer gave the average temperature of a pressure tube along the span of the blade which was recorded simultaneously with the pressures on every test point.

The pressure tubes were brought out of the blade surface inside a rotating spinner and run through the hollow dynamometer shaft to the transfer device mounted in the rear. A schematic diagram of the test setup is shown in figure 1.

TESTS

The tests were made at values of blade angle of 30° and 45° at the 75-percent (45 in.) radius station. A constant rotational speed was used for each test and a range of advance ratio was covered by changing the tunnel airspeed, which was varied from about 60 to 460 miles per hour. At a blade angle of 45°, however, the dynamometer could not deliver sufficient torque to cover the complete range of advance ratio at the higher rotational speeds and for this reason high-speed data were obtained by operating the tunnel at constant high values of airspeed and variable dynamometer rotational speeds.

Running the tests as described, the section Mach number and the section nominal angle of attack were varied simultaneously, the latter varying over a fairly large range and the section Mach number varying over a small range. Since the nominal angle of attack is a function of advance ratio at constant blade angle, a Mach number range was

UNCLASSIFIED

UNCLASSIFIED

covered by running the tests over the same range of advance ratio a number of times using a different combination of tunnel airspeed and rotational speed. The Mach number range covered for the outboard stations was from about 0.6 to 1.1, and for the inboard stations from about 0.3 to 0.6. The nominal angle-of-attack range varied from about -1° to 12° for low values of Mach number and from about 0° to 4° for the higher values of Mach number.

During the tests force measurements of propeller thrust and torque together with slipstream survey measurements were made simultaneously with the measurement of the section pressure distribution.

In order to make available as much data as possible at the earliest date possible, complete analysis has been deferred and this paper prepared to present only the data obtained by measuring the pressure distribution on the blade sections over the complete Mach number range tested for values of nominal angle of attack of 0° to 4°.

REDUCTION OF DATA

Symbols.- The symbols used throughout this report, some of which are defined in figure 3, are as follows:

b	blade chord, feet
c	distance from section leading edge to any point on the chord, feet
$\bar{c}$	distance from section leading edge to any point about which moments are taken, feet
c_{l_d}	design lift coefficient
c_m	section moment coefficient
c_n	section normal-force coefficient
D	propeller diameter, feet
F_n	section normal force
g	acceleration due to gravity, 32.2 ft/sec^2
h	blade section maximum thickness, feet
J	advance ratio (V/nD)

UNCLASSIFIED CONFIDENTIAL

K	gas constant, 53.3 ft-lb/lb/°F
M	free-stream Mach number
M_x	helical section Mach number $\left(M\sqrt{1+\left(\frac{\pi x}{J}\right)^2}\right)$
m	section moment, pound-feet
N	propeller rotational speed, rpm
n	propeller rotational speed, rps
P_x	pressure coefficient at a radial station x $\left(\frac{p-p_o}{q_x}\right)$
p	station pressure, lbs/sq ft
p_m	static pressure as read on manometer board (uncorrected for centrifugal pressure), lbs/sq ft
p_o	free-stream static pressure, lbs/sq ft
q_x	resultant dynamic pressure at a radial station x, lbs/sq ft $\left(\frac{1}{2}\rho V_x^2\right)$
R	propeller-tip radius, feet
r	radius to a blade element, feet
r_1	radius to orifice in rotating shaft of pressure-transfer device, feet
$\bar{T}$	absolute mean temperature of air in propeller tubing, °F abs.
V	free-stream velocity, ft/sec
V_x	resultant velocity at a radial station x, ft/sec $\left(V\sqrt{1+\left(\frac{\pi x}{J}\right)^2}\right)$
W	true resultant velocity, ft/sec
w_1	induced velocity, ft/sec
x	radial distance to a blade element (r/R)

α_x angle of attack of blade element, corrected for induced flow, at radial station x, degrees $(\beta - \phi)$

α_x' nominal angle of attack of blade element at radial station x, degrees $(\beta - \phi_o)$

β blade angle, degrees

ϵ induced angle of attack

ρ mass density of air in free stream, slugs per cubic foot

ϕ helix angle

ϕ_o nominal helix angle $\left(\tan^{-1}\left(J/\pi x\right)\right)$

ω propeller rotational speed, radians/sec

Pressure coefficient.- The pressure coefficient for a pressure measured on the surface of the propeller blade is defined as the difference between the measured surface pressure and the free-stream static pressure immediately ahead of the propeller, divided by the resultant section dynamic pressure, so that

$$P_x = \frac{p - p_o}{q_x}$$

The effect of the rotation of the propeller section is to change the section velocity and total pressure, but the static pressure and mass density of the air remain the same as for the free air stream.

The pressure p at a point on the blade surface is the pressure recorded on the manometer corrected for the centrifugal force on the air column in the pressure tube due to the rotation of the blade, so that

$$p = p_m \rho^{\frac{\omega^2}{2gKT}\left(r^2 - r_1^2\right)}$$

This relation is explained in reference 2. For the present installation r_1 was small compared with r and was called zero with negligible effect on the resulting pressure coefficient.

Normal-force coefficient.- The normal-force coefficient of a section is defined as the normal force acting on a section of unit

UNCLASSIFIED

faired mean line drawn through the test points and the values so read are the values shown by symbols on the plots. The data presented in figures 5 through 22 are to be regarded as preliminary insofar as they have been obtained by a fairing process; they include effects of propeller blade deflection; and they have not been corrected for the induced angle.

A comparison is made in figure 23 of normal-force coefficient, obtained on the propeller at the 80-percent-radius station with the lift coefficient corrected for tunnel blockage obtained from two-dimensional tests on approximately the same section in the Langley 24-inch high-speed tunnel (unpublished data). The data are compared for low values of angle of attack so that the difference between normal-force coefficient and lift coefficient is very small. The angle of attack of the propeller section in this figure has been corrected for induced flow; therefore, the angles of attack for which the propeller-section data are presented are comparable with angles for the two-dimensional data.

Figure 24 shows a comparison of the section moment coefficient about the quarter-chord point obtained on the propeller section with two-dimensional-tunnel data. The angles of attack for the propeller data shown in this figure have also been corrected for induced flow.

These comparisons give an idea of the changes that may occur in the section characteristics when the section is incorporated in a propeller blade to operate at high speed. These changes are particularly apparent near the propeller blade tip when the section is operating above its two-dimensional critical speed.

Langley Memorial Aeronautical Laboratory
National Advisory Committee for Aeronautics
Langley Field, Va.

UNCLASSIFIED

span divided by the chord of the section and the resultant section dynamic pressure, thus,

$$c_n = \frac{F_n}{q_x b} = \int_0^{1.0} P_x \, d\frac{c}{b}$$

Moment coefficient.— The moment coefficient of a section is defined as:

$$c_m = \frac{m}{q_x b^2} = \frac{\bar{c}}{b} \int_0^{1.0} P_x \, d\frac{c}{b} - \int_0^{1.0} P_x \frac{c}{b} \, d\frac{c}{b}$$

A positive value of moment coefficient is defined as a moment tending to increase the section angle of attack. In this report the moments were taken about the section quarter-chord point so that $\frac{\bar{c}}{b} = 0.25$.

RESULTS

As a preliminary check on the functioning of the test apparatus a comparison of a pressure-distribution diagram obtained on the propeller at the 80-percent-radius station is compared with the theoretical pressure distribution in figure 4. The experimental data are preliminary and the normal force has not been reduced to lift so that the comparison in figure 4 is only approximately at the same value of lift coefficient. However, the values chosen are considered close enough to verify the validity of the experimental data. The agreement is very good over most of the section. There is a discrepancy near the leading edge but this discrepancy has been found in other tunnel work and may be due to the sensitivity of the theory to slight changes in curvature near the leading edge.

Plots of section normal-force coefficient and section moment coefficient about the one-quarter-chord point versus section Mach number are presented in figures 5 through 22 at values of nominal section angle of attack of 0°, 1°, 2°, 3°, and 4° for the nine radial stations tested. The blade section design parameters are given in table I.

The tests were run by first increasing and then decreasing the advance ratio. The data presented herein are values read from a

UNCLASSIFIED

REFERENCES

1. Corson, Blake W., Jr., and Maynard, Julian D.: The NACA 2000-Horsepower Propeller Dynamometer and Tests at High Speed of an NACA 10-(3)(08)-03 Two-Blade Propeller. NACA RM No. L7L29, 1948

2. Runckel, Jack F., and Davey, Richard S.: Pressure-Distribution Measurements on the Rotating Blades of a Single-Stage Axial-Flow Compressor. NACA TN No. 1189, 1947.

UNCLASSIFIED

UNCLASSIFIED

TABLE I

SECTION DESIGN CHARACTERISTICS FOR THE

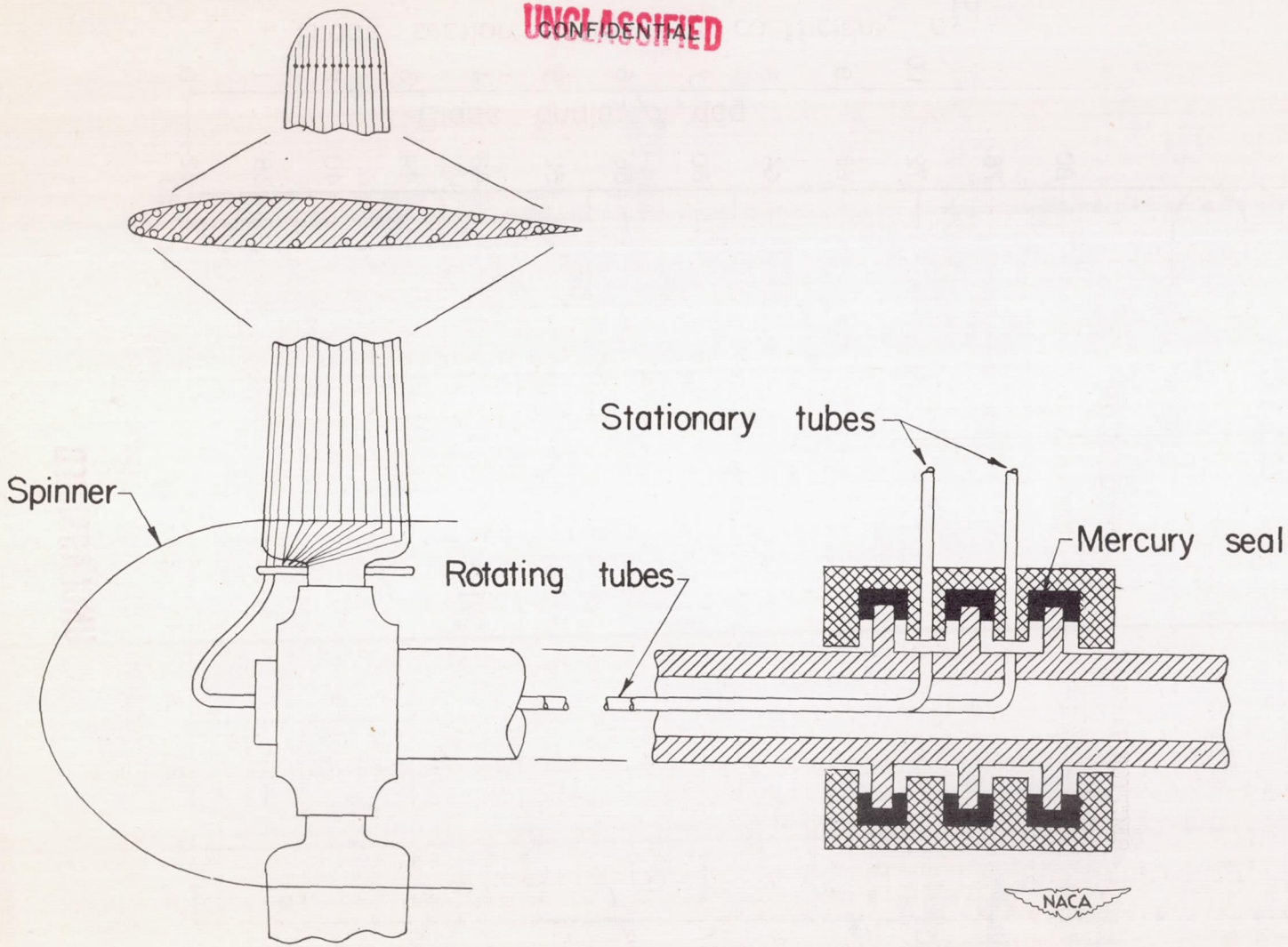
NACA 10-(3)(08)-03 PROPELLER BLADE

Figure number	Radial station $r = \frac{r}{R}$	Section chord, b (ft)	Design lift coefficient c_{l_d}	Thickness ratio h/b	Section twist $\beta_x - \beta_{0.75R}$ (deg)
5, 14	0.30	0.931	0.143	0.130	23.45
6, 15	.45	.829	.228	.1085	14.93
7, 16	.60	.727	.282	.0905	6.25
8, 17	.70	.657	.297	.0800	1.98
9, 18	.75	.623	.300	.0745	0
4, 10, 19, 23, 24	.80	.589	.295	.0695	-1.82
11, 20	.85	.555	.282	.0643	-3.52
12, 21	.90	.520	.252	.0577	-5.12
13, 22	.95	.473	.203	.0476	-6.67

NACA

UNCLASSIFIED

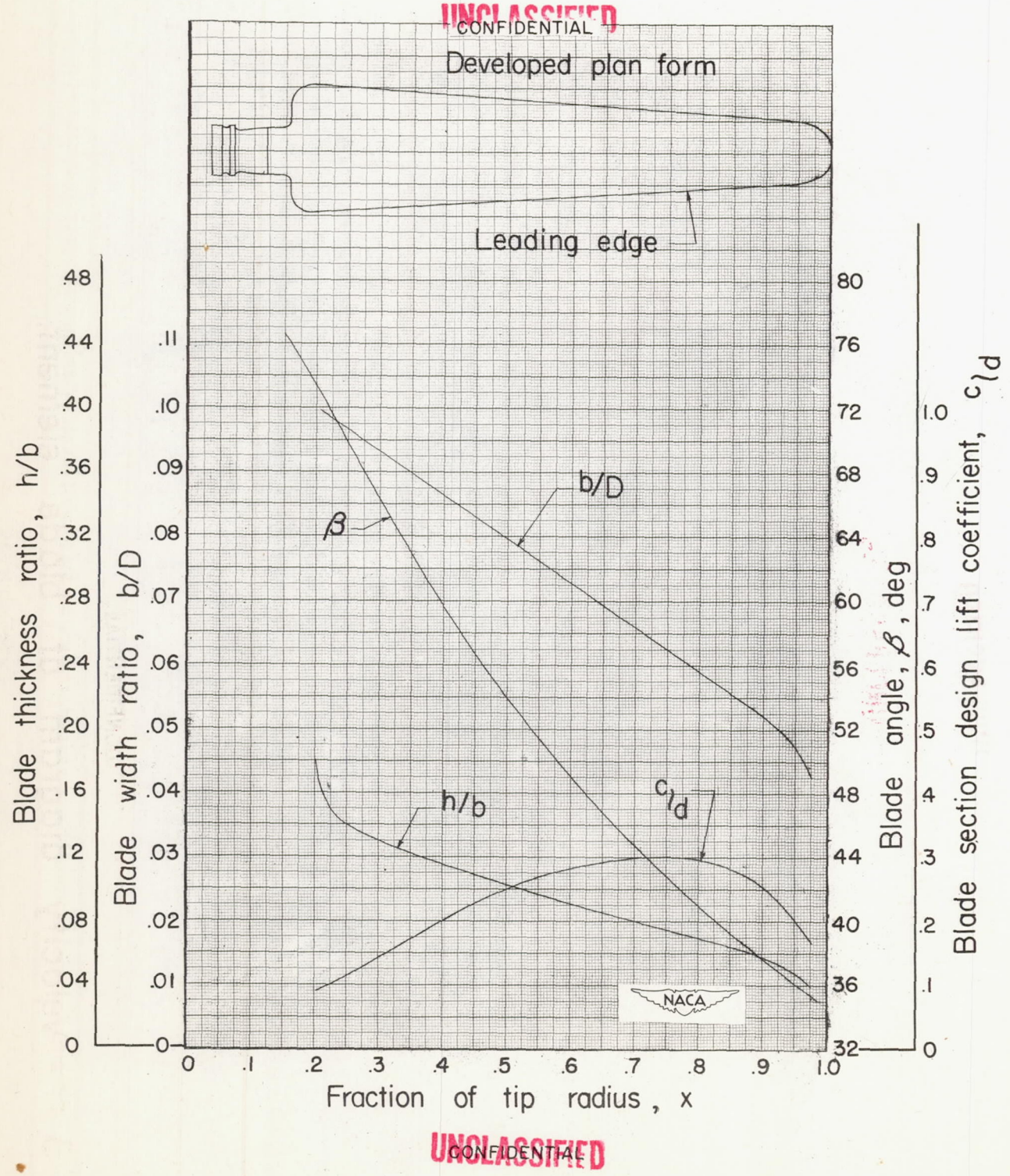
UNCLASSIFIED
CONFIDENTIAL



CONFIDENTIAL

Figure 1. — Schematic diagram showing method of measuring pressures.

UNCLASSIFIED
CONFIDENTIAL



UNCLASSIFIED
CONFIDENTIAL

Figure 2. — Blade-form curves for NACA 10-(3)(08)-03 propeller.

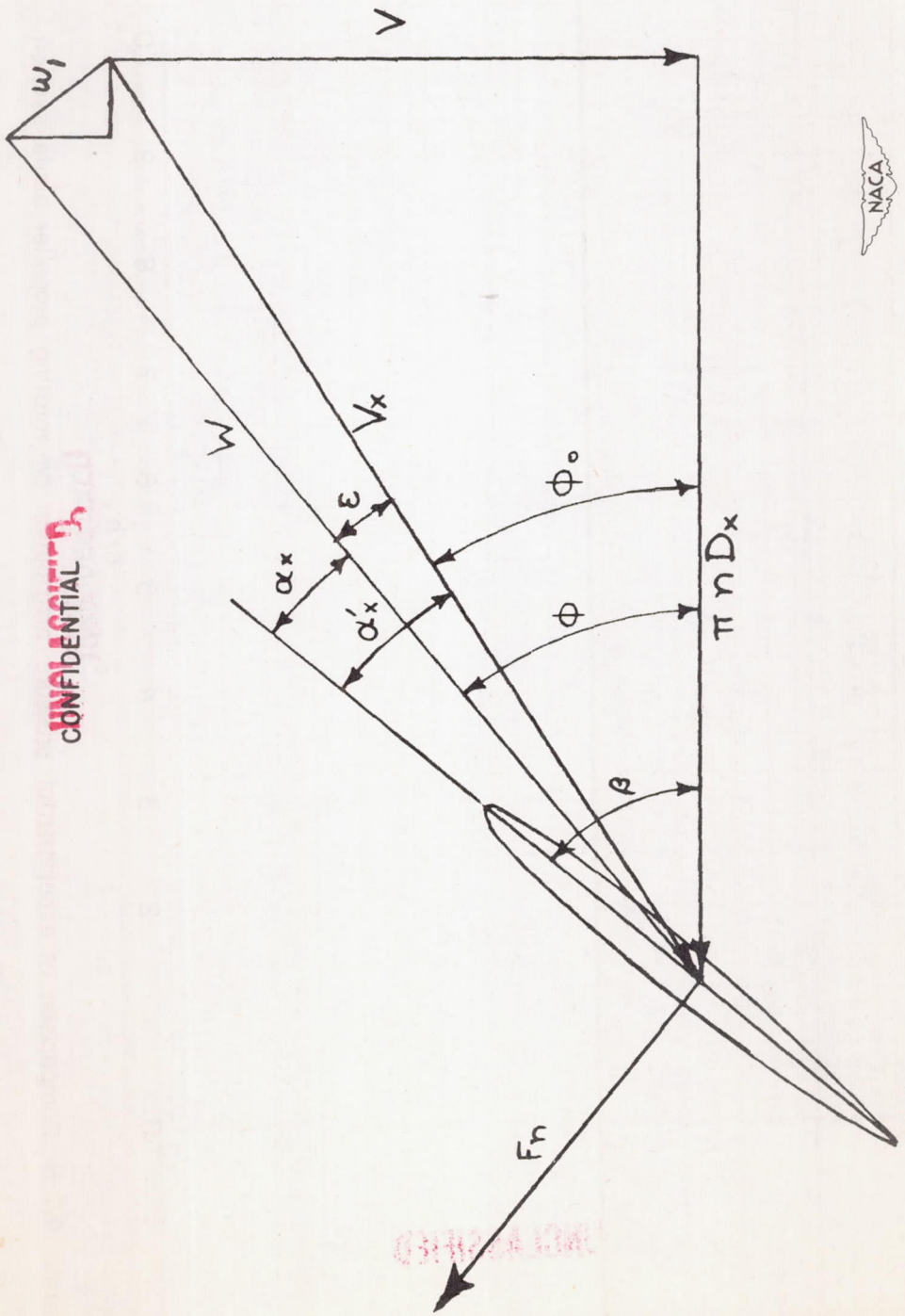


Figure 3.—Velocity diagram at blade element.

CONFIDENTIAL
UNCLASSIFIED

UNCLASSIFIED

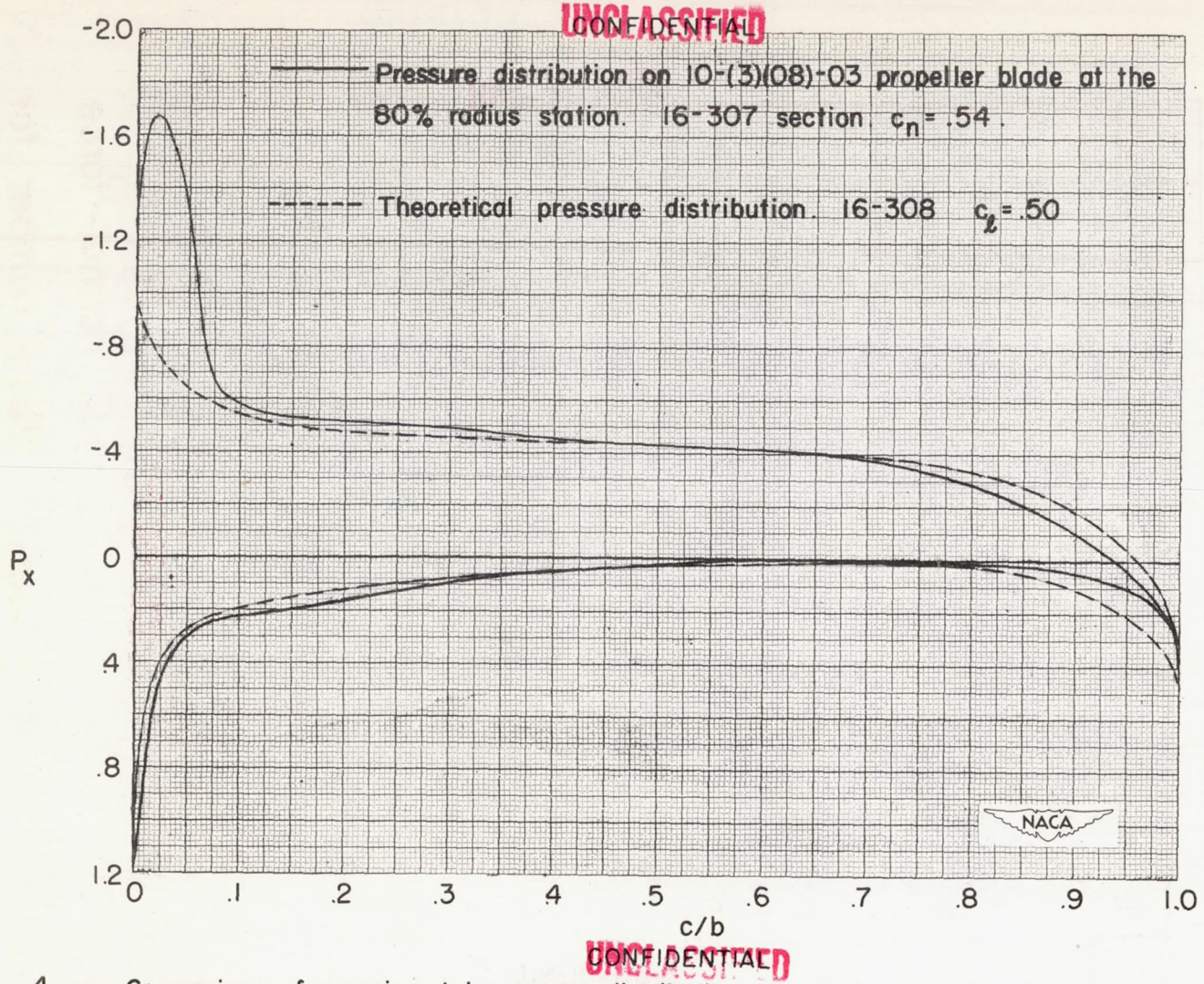
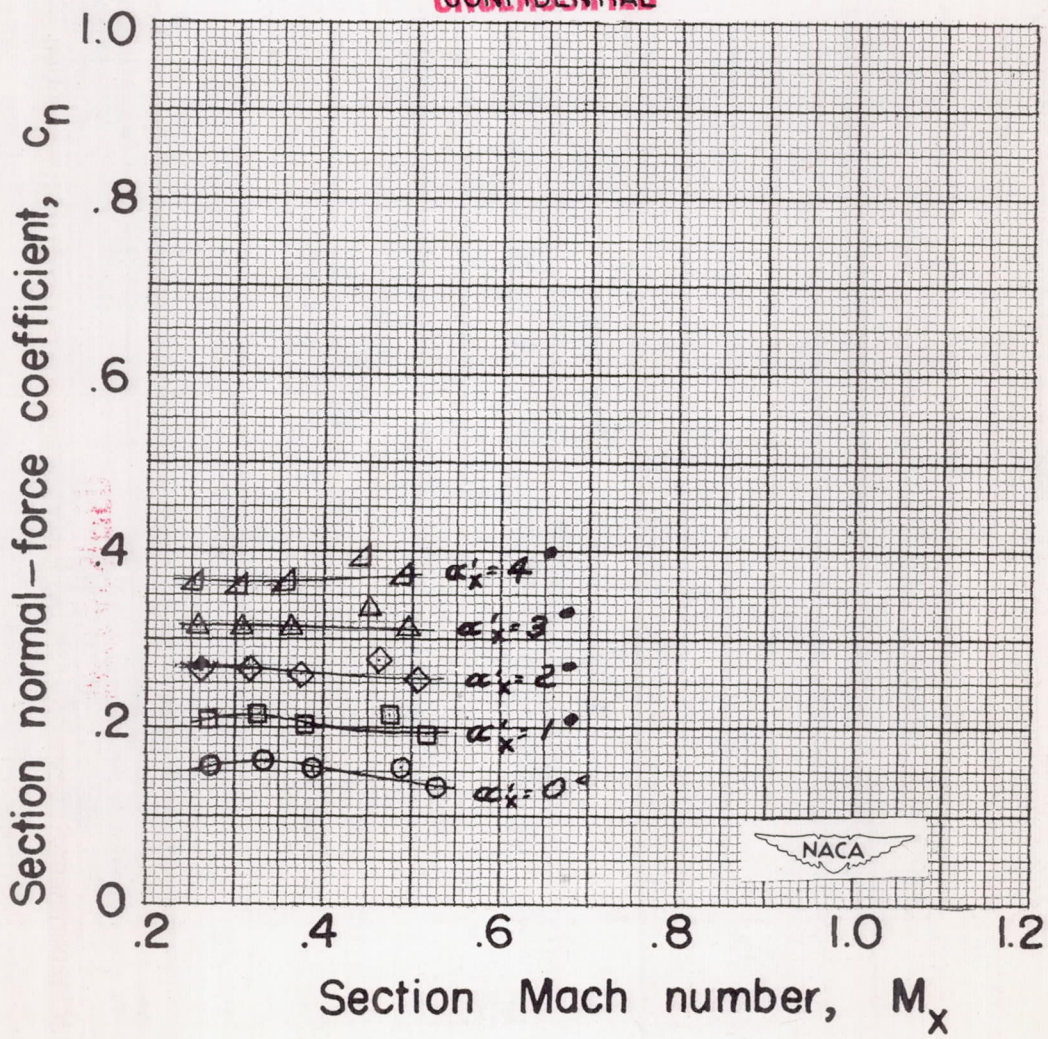


Figure 4. — Comparison of experimental pressure distribution on rotating propeller blade section with theoretical pressure distribution.

UNCLASSIFIED
CONFIDENTIAL

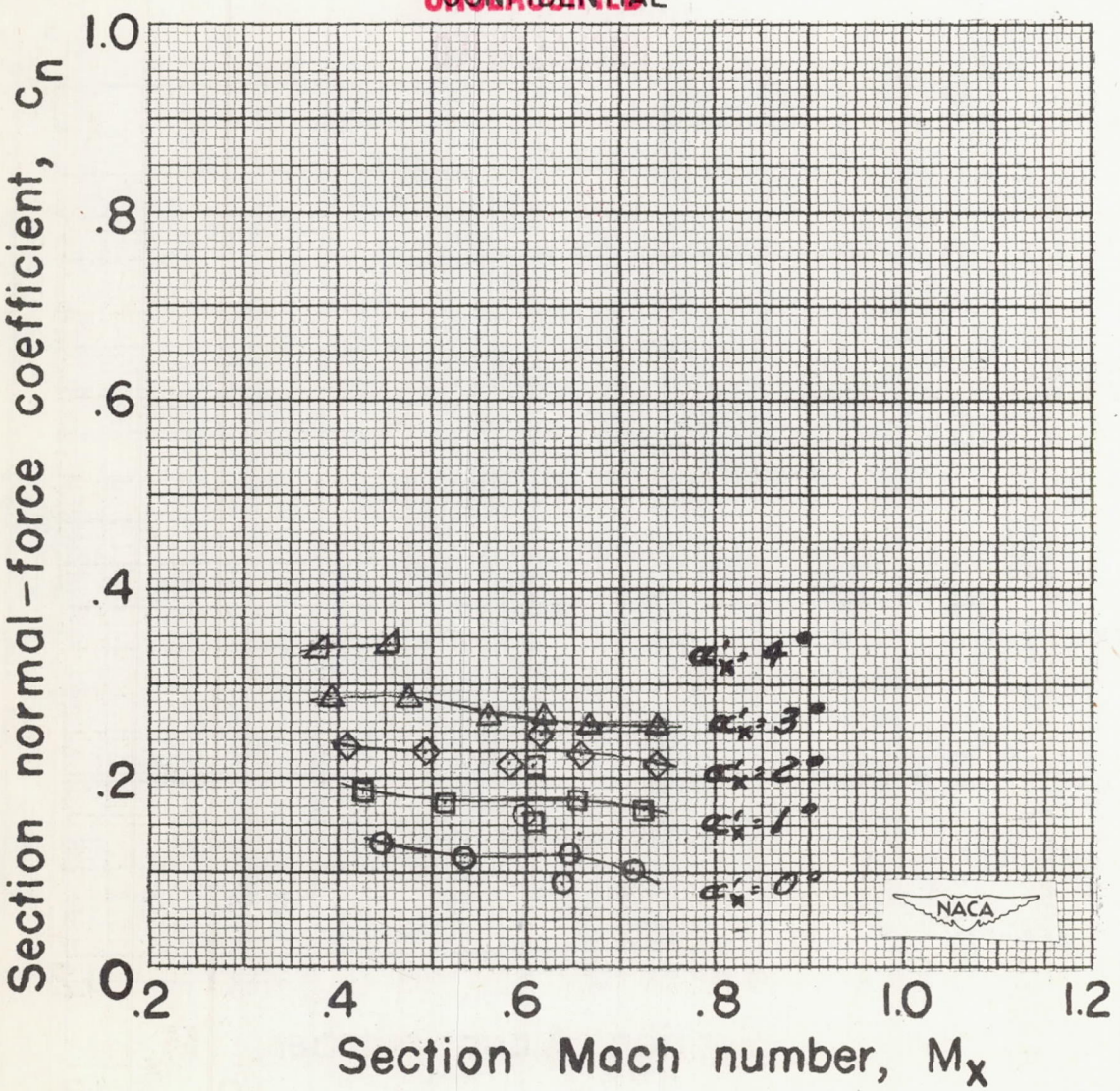


(a) $\beta_{0.75R} = 30°$.

CONFIDENTIAL
UNCLASSIFIED

Figure 5.—Variation of section normal-force coefficient with section Mach number for several angles of attack. Radial station = 0.3.

UNCLASSIFIED
CONFIDENTIAL

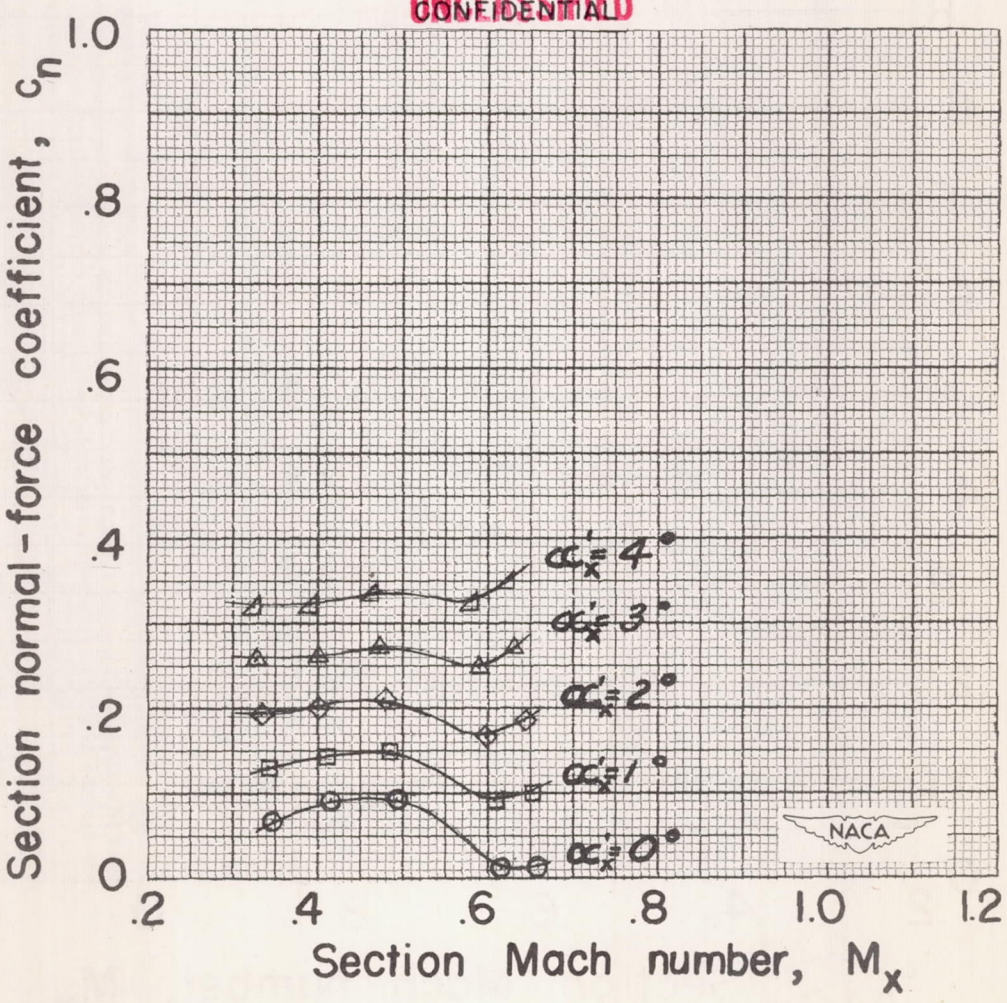


(b) $\beta_{0.75R} = 45°$.

UNCLASSIFIED
CONFIDENTIAL

Figure 5. — Concluded.

UNCLASSIFIED
CONFIDENTIAL

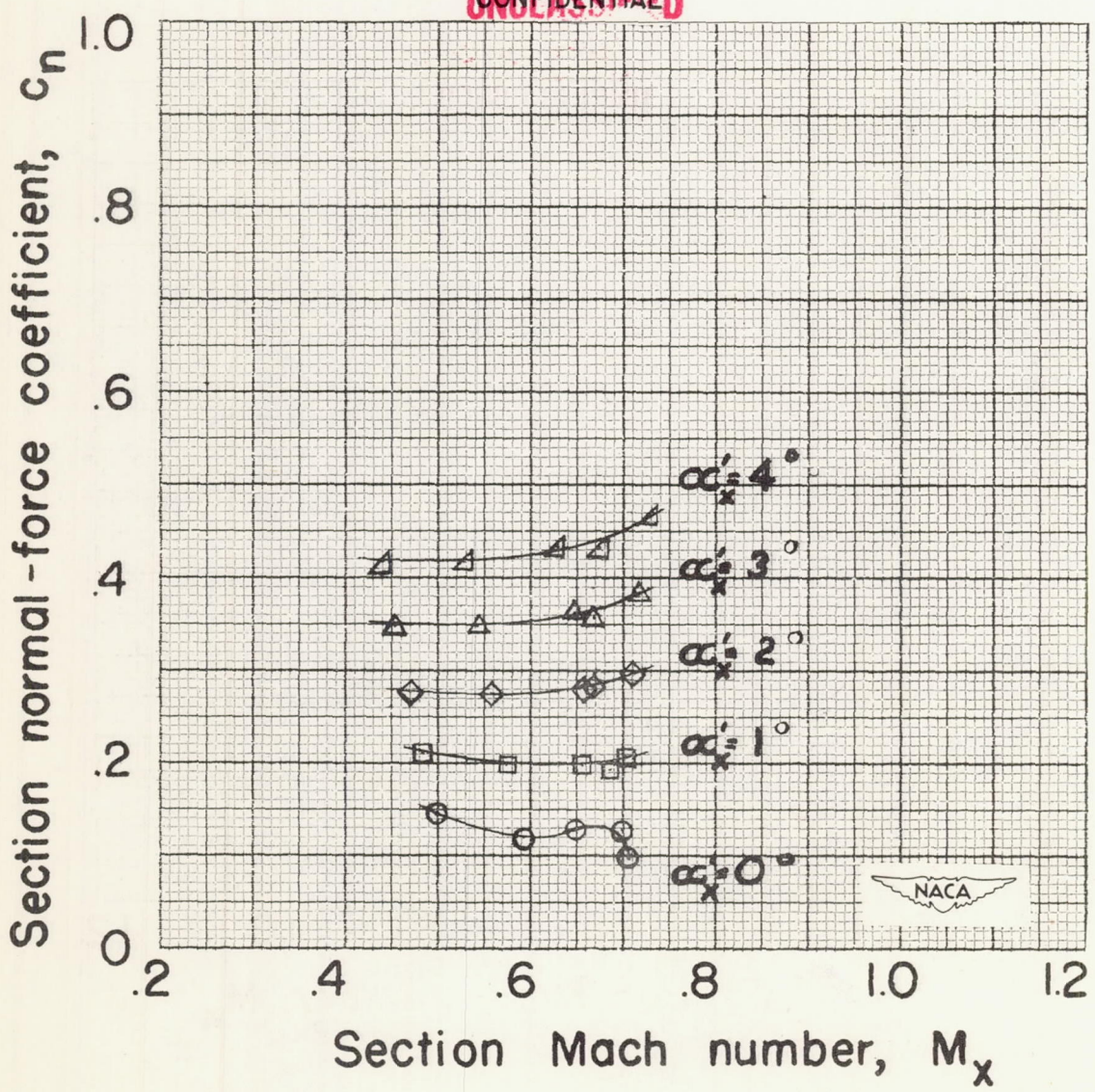


(a) $\beta_{0.75R} = 30°$.

CONFIDENTIAL
UNCLASSIFIED

Figure 6.—Variation of section normal-force coefficient with section Mach number for several angles of attack. Radial station = 0.45.

UNCLASSIFIED
CONFIDENTIAL

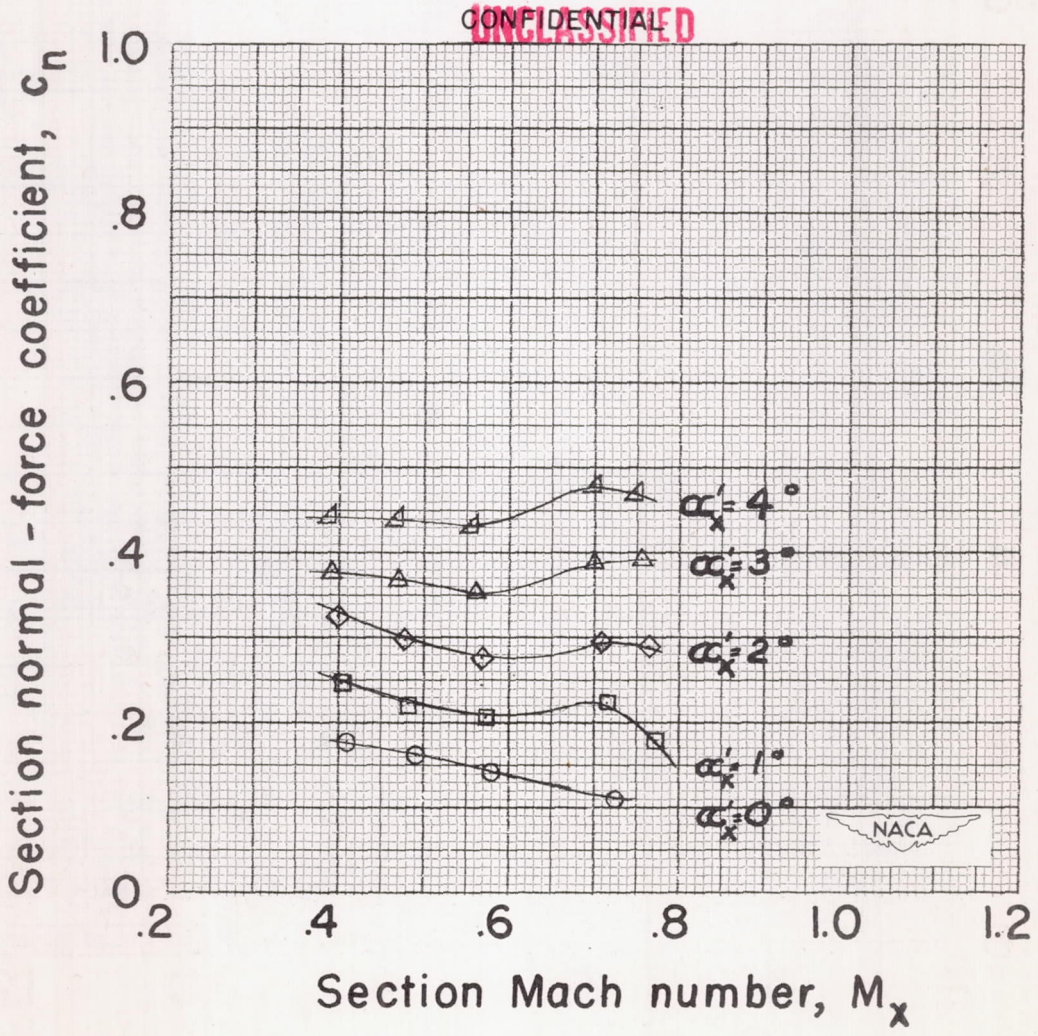


(b) $\beta_{0.75R} = 45°$.

UNCLASSIFIED
CONFIDENTIAL

Figure 6. — Concluded.

CONFIDENTIAL UNCLASSIFIED

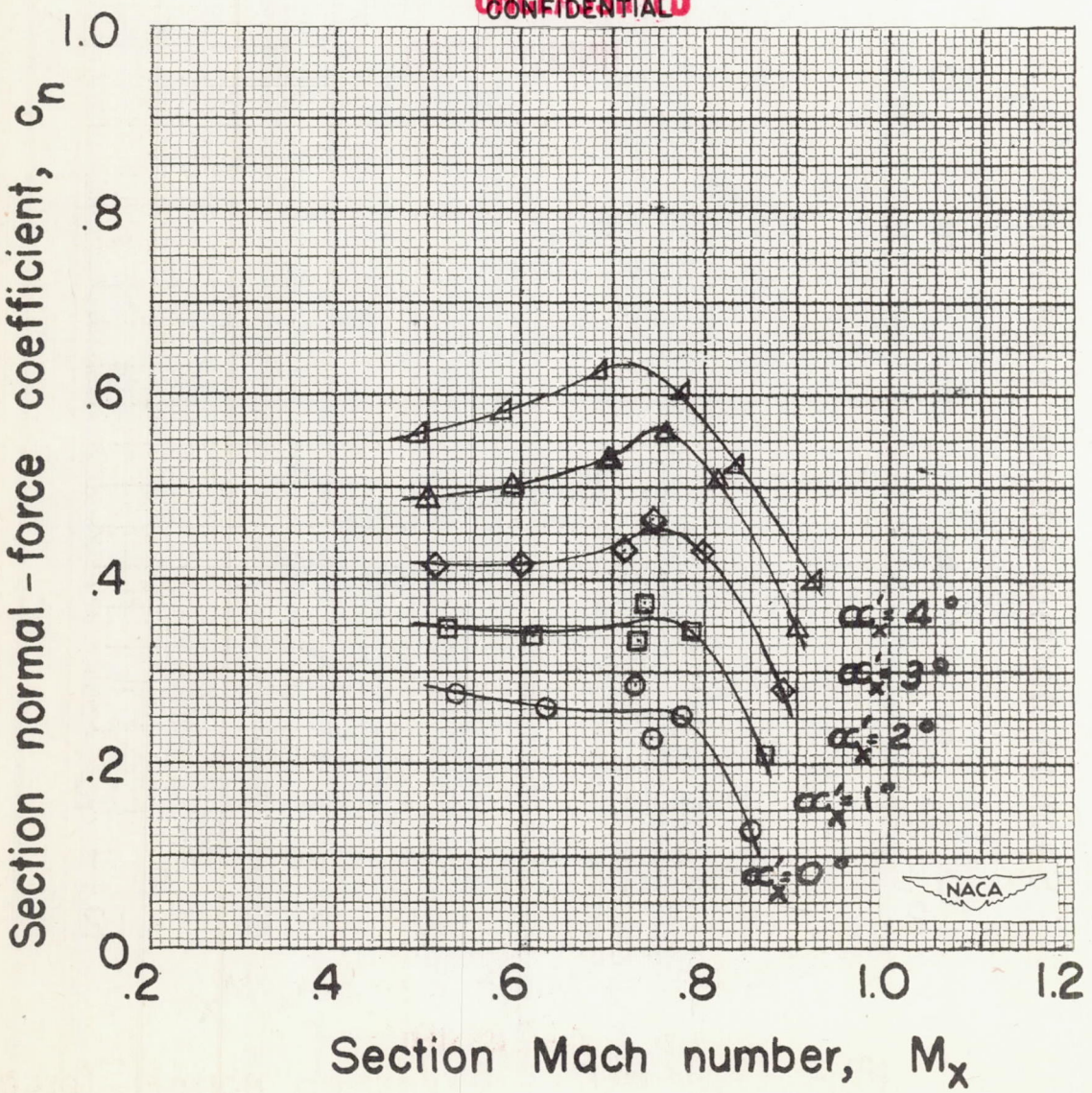


(a) $\beta_{0.75R} = 30°$

CONFIDENTIAL UNCLASSIFIED

Figure 7. —Variation of section normal-force coefficient with section Mach number for several angles of attack. Radial station = 0.60.

UNCLASSIFIED
CONFIDENTIAL

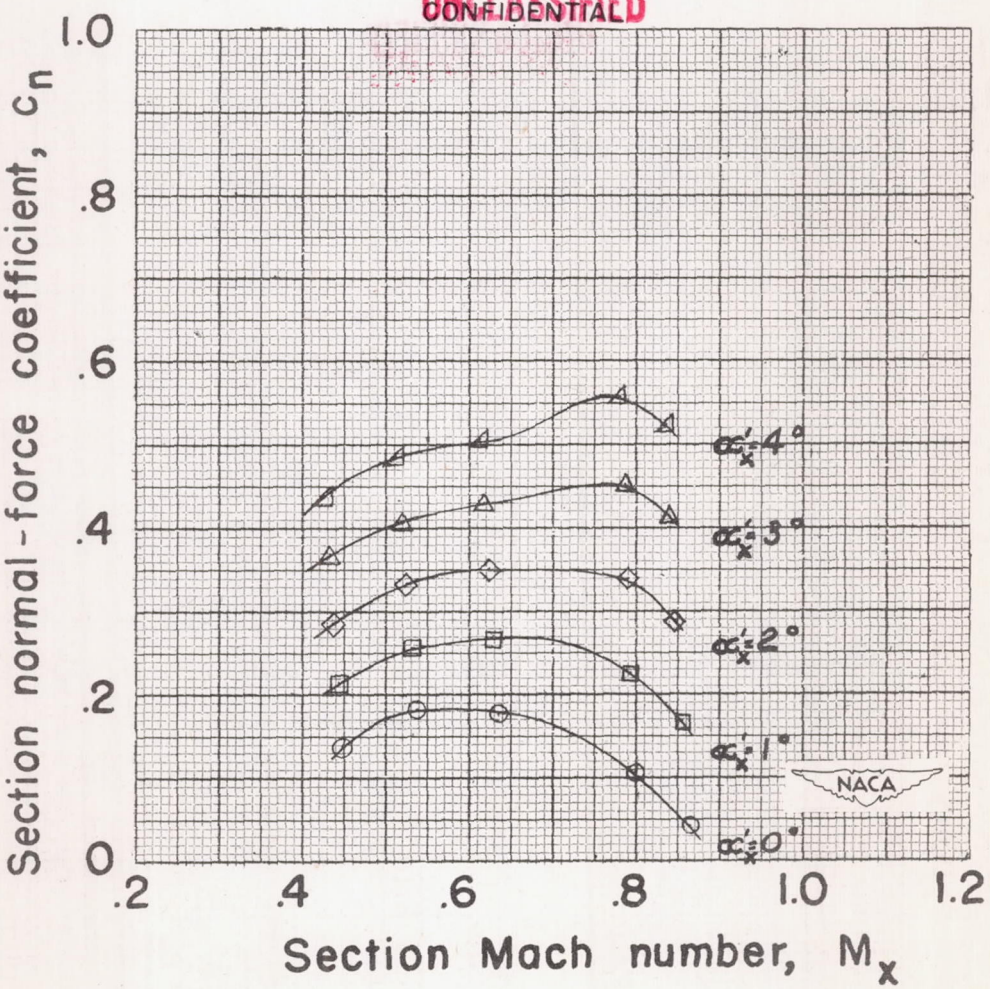


(b) $\beta_{0.75R} = 45°$.

CONFIDENTIAL
UNCLASSIFIED

Figure 7. — Concluded.

UNCLASSIFIED
CONFIDENTIAL

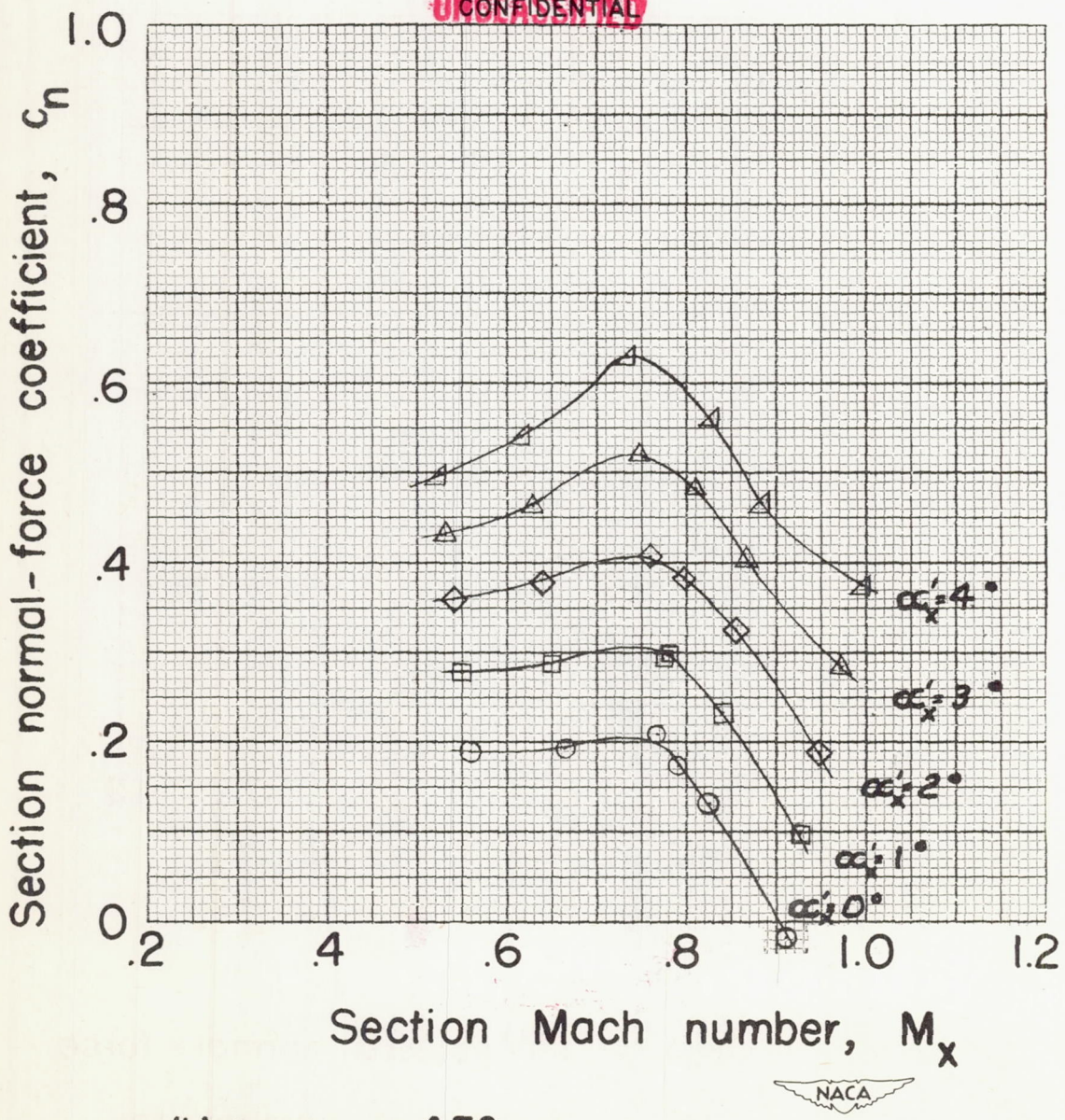


(a) $\beta_{0.75R} = 30°$.

UNCLASSIFIED
CONFIDENTIAL

Figure 8. —Variation of section normal-force coefficient with section Mach number for several angles of attack. Radial station=0.7.

UNCLASSIFIED
CONFIDENTIAL

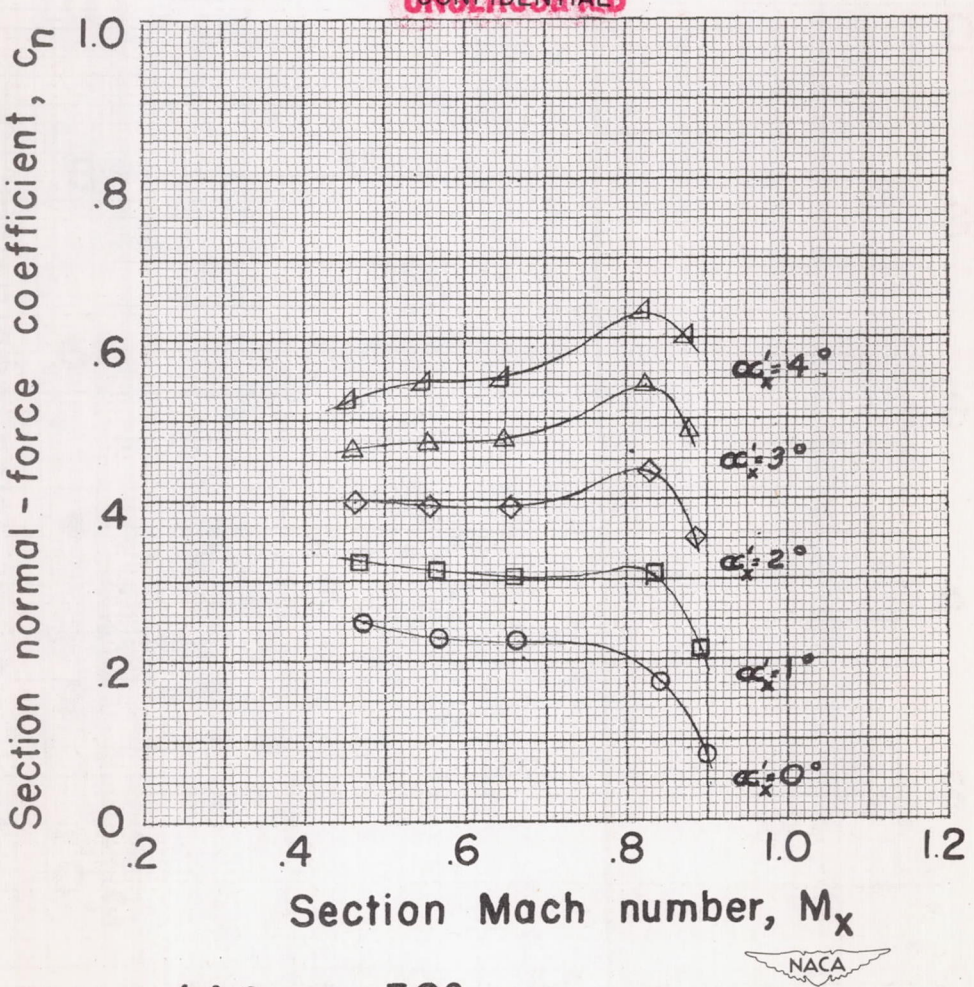


(b) $\beta_{0.75R} = 45°$.

UNCLASSIFIED
CONFIDENTIAL

Figure 8. — Concluded.

UNCLASSIFIED
CONFIDENTIAL

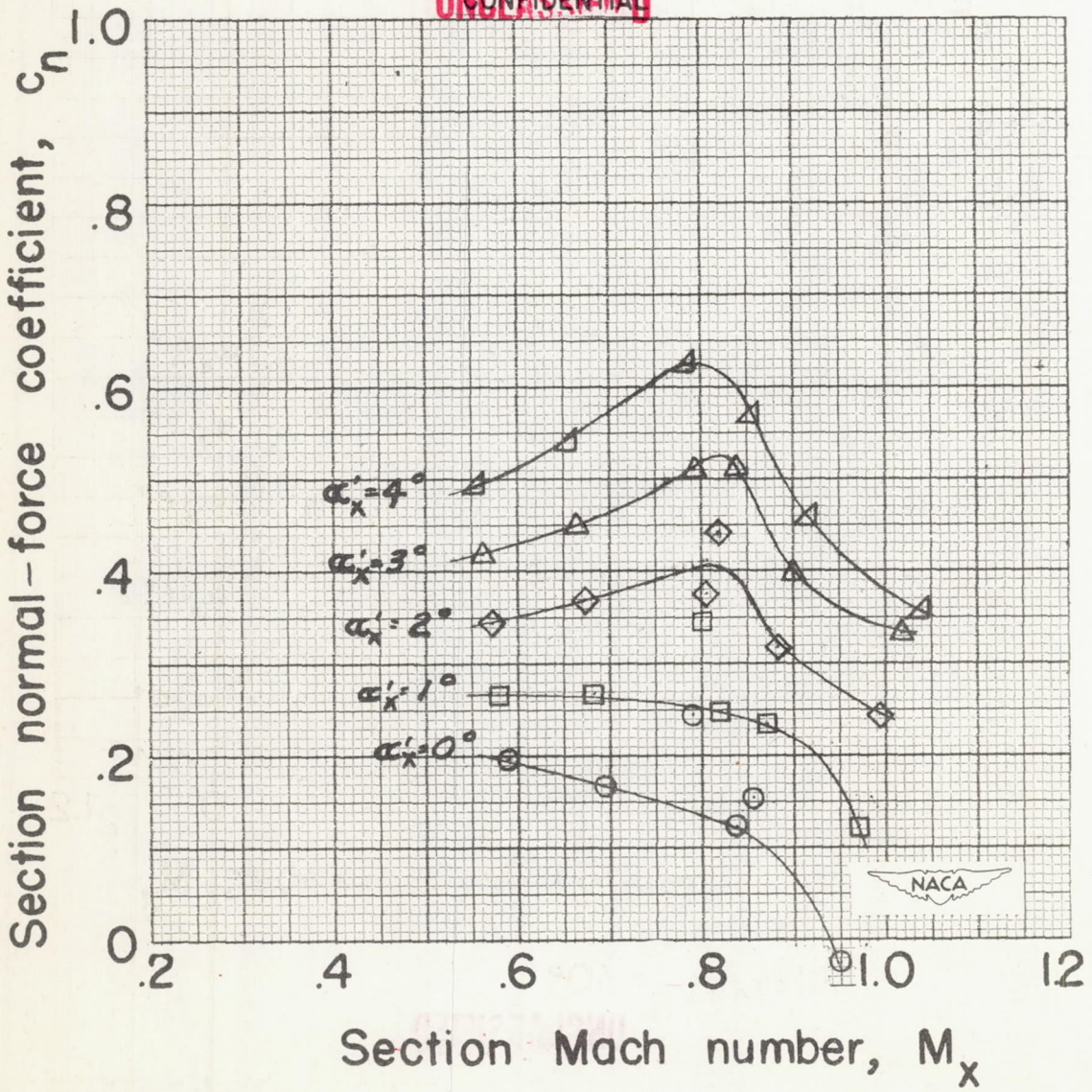


(a) $\beta_{0.75R} = 30°$

UNCLASSIFIED
CONFIDENTIAL

Figure 9. —Variation of section normal - force coefficient with section Mach number for several angles of attack. Radial station = 0.75.

UNCLASSIFIED CONFIDENTIAL

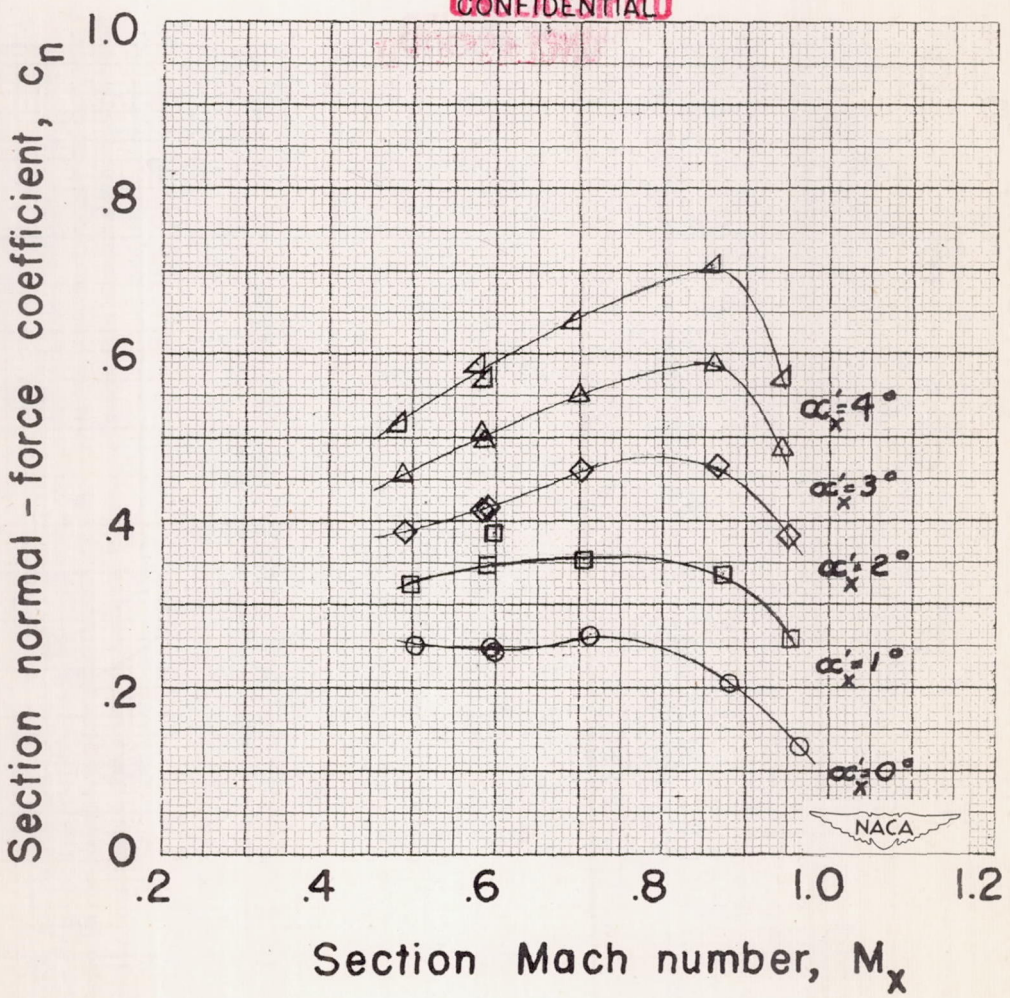


(b) $\beta_{0.75R} = 45°$.

UNCLASSIFIED CONFIDENTIAL

Figure 9. — Concluded.

UNCLASSIFIED
CONFIDENTIAL

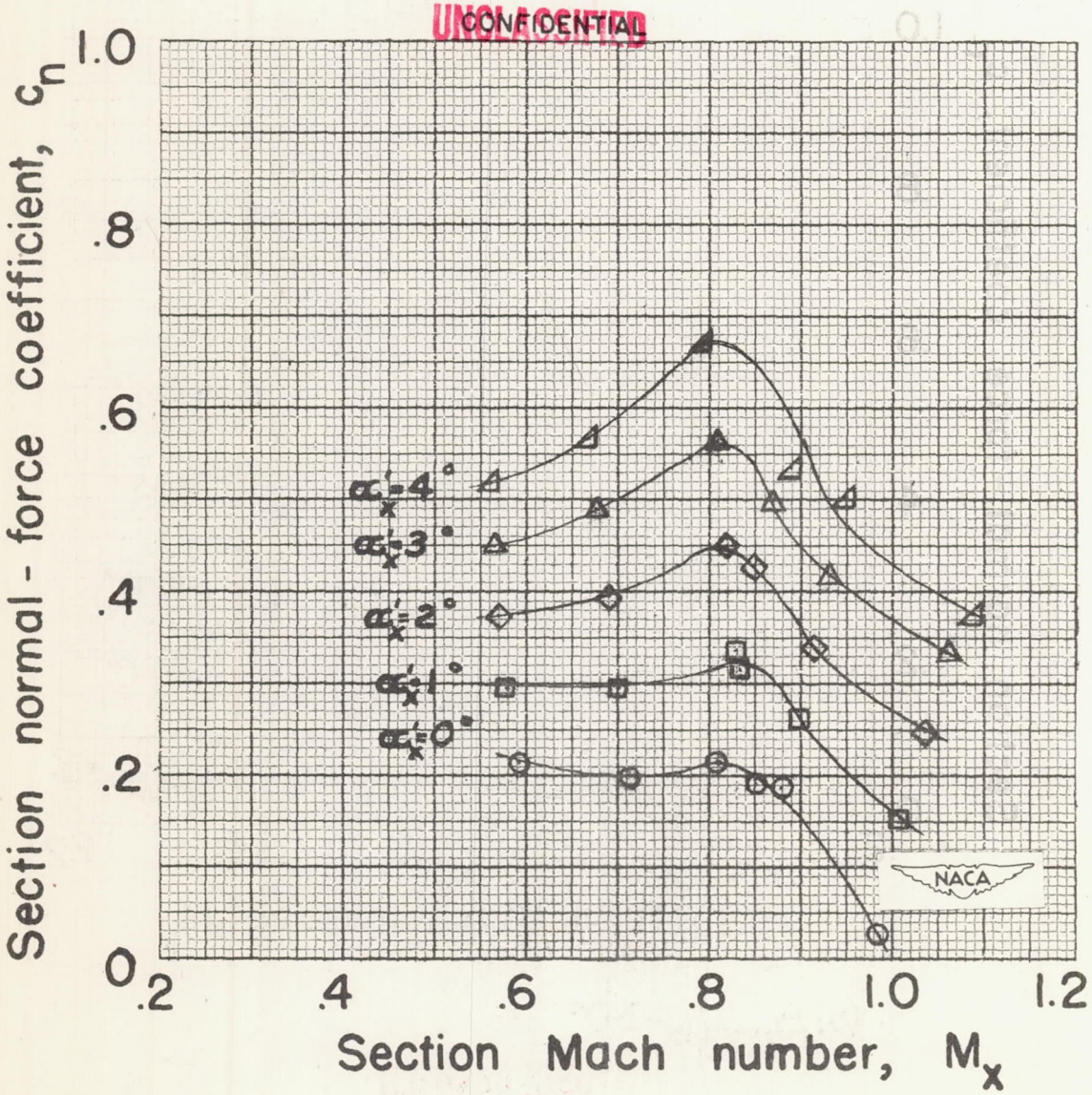


(a) $\beta_{0.75R} = 30°$

UNCLASSIFIED
CONFIDENTIAL

Figure 10.—Variation of section normal-force coefficient with section Mach number for several angles of attack. Radial station=0.8.

UNCLASSIFIED

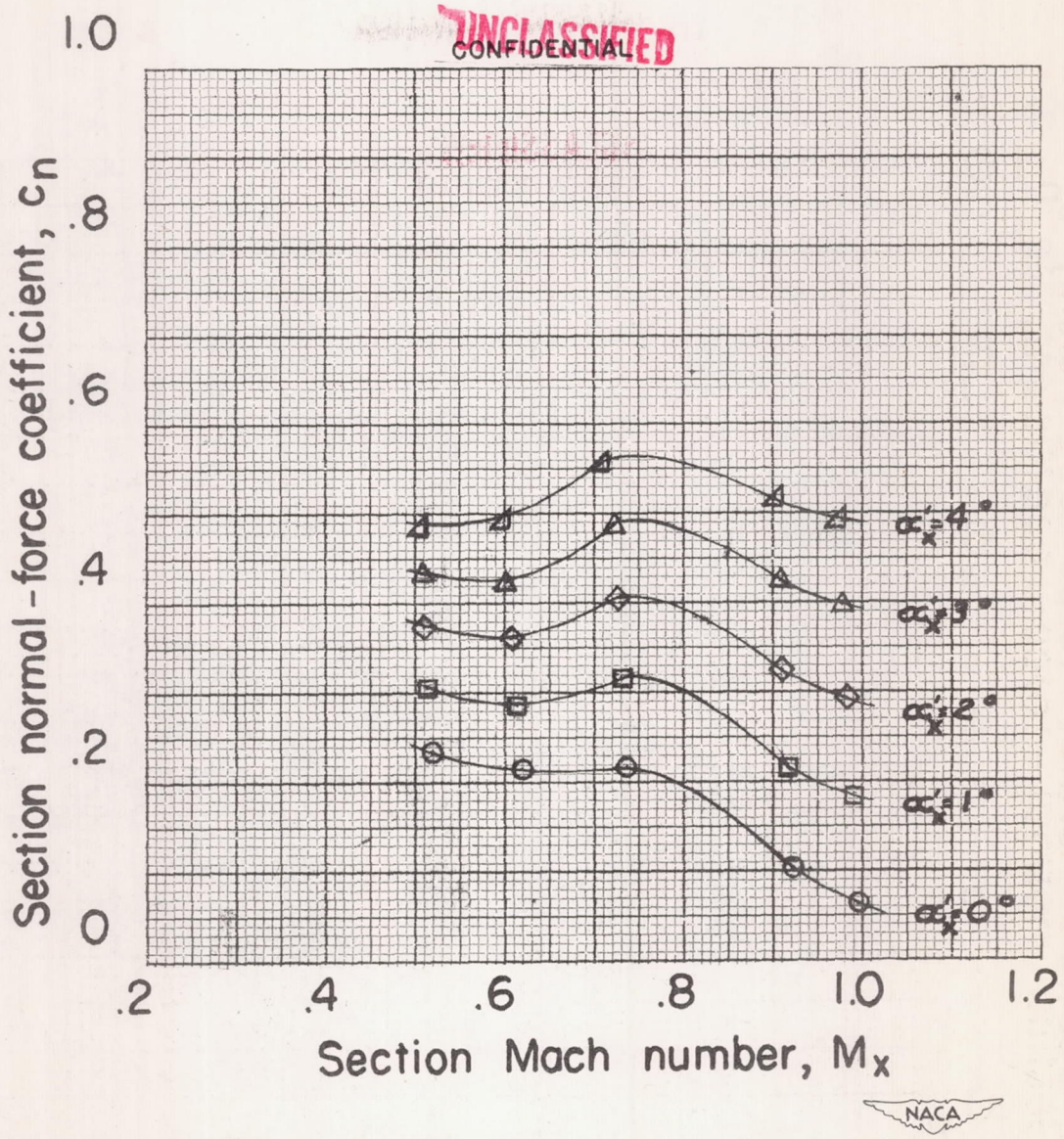


(b) $\beta_{0.75R} = 45°$.

UNCLASSIFIED
CONFIDENTIAL

Figure 10 .— Concluded.

UNCLASSIFIED
CONFIDENTIAL



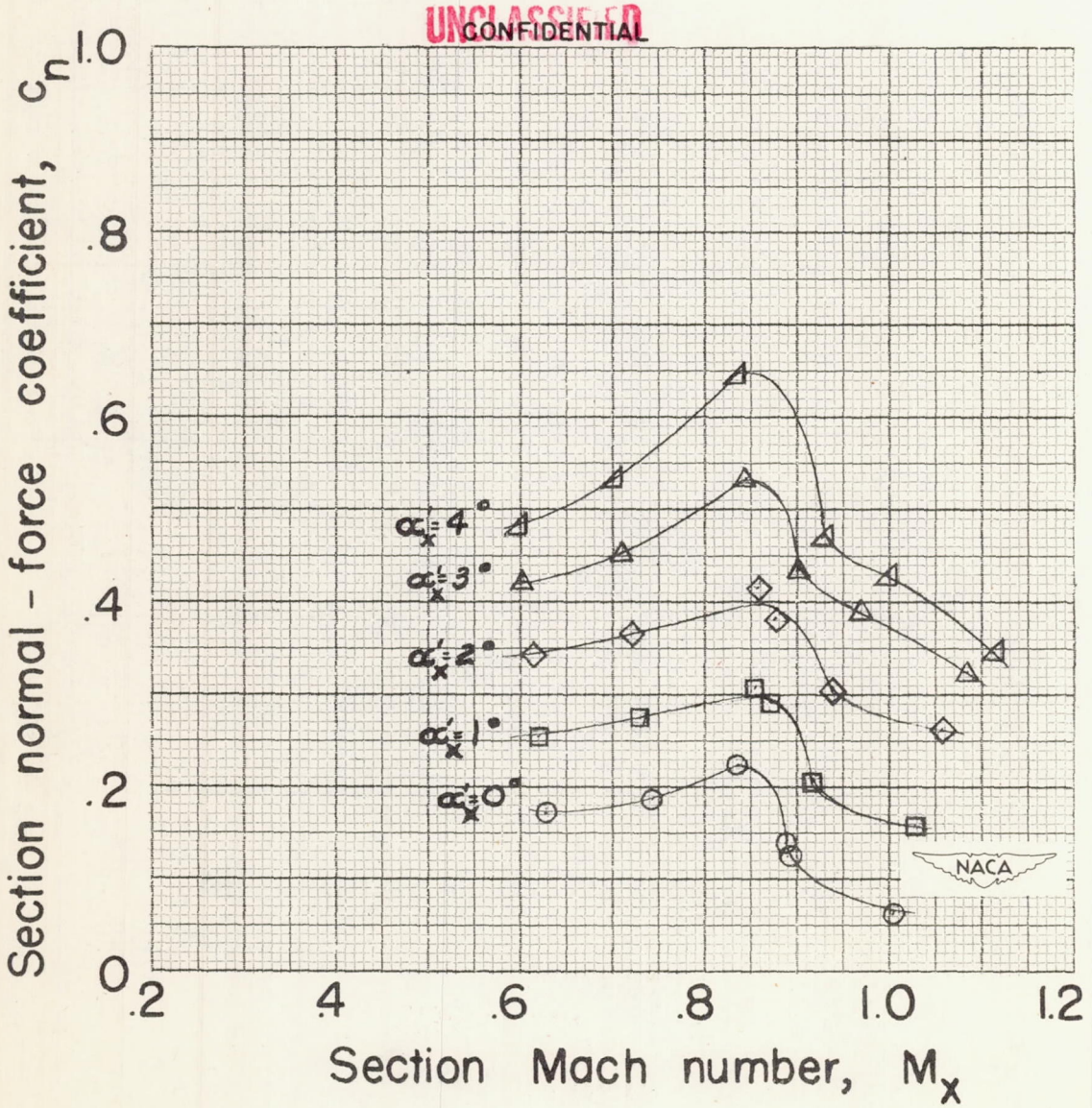
(a) $\beta_{0.75R} = 30°$.

UNCLASSIFIED
CONFIDENTIAL

Figure 11.—Variation of section normal-force coefficient with section Mach number for several angles of attack. Radial station = 0.85.

CONFIDENTIAL

UNCLASSIFIED



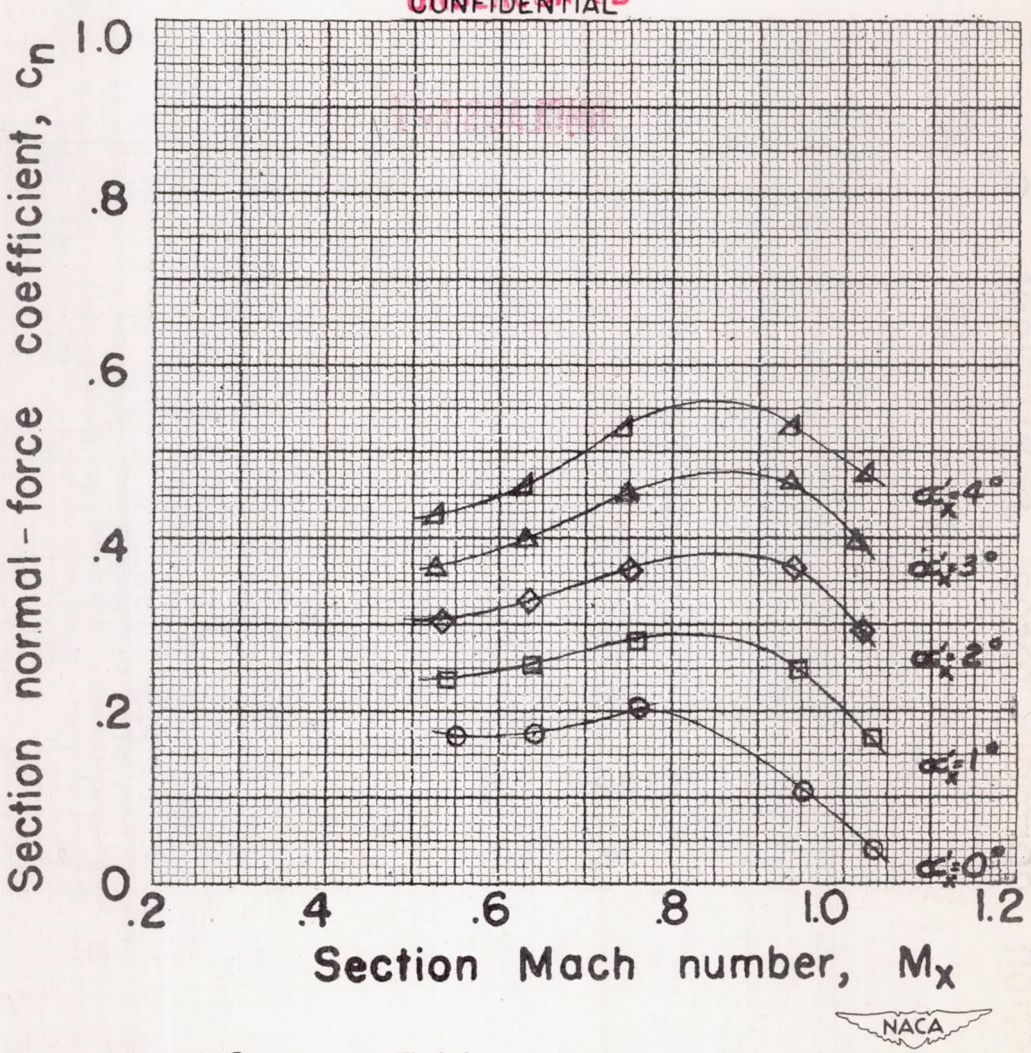
(b) $\beta_{0.75R} = 45°$.

CONFIDENTIAL

UNCLASSIFIED

Figure 11 .— Concluded.

UNCLASSIFIED
CONFIDENTIAL

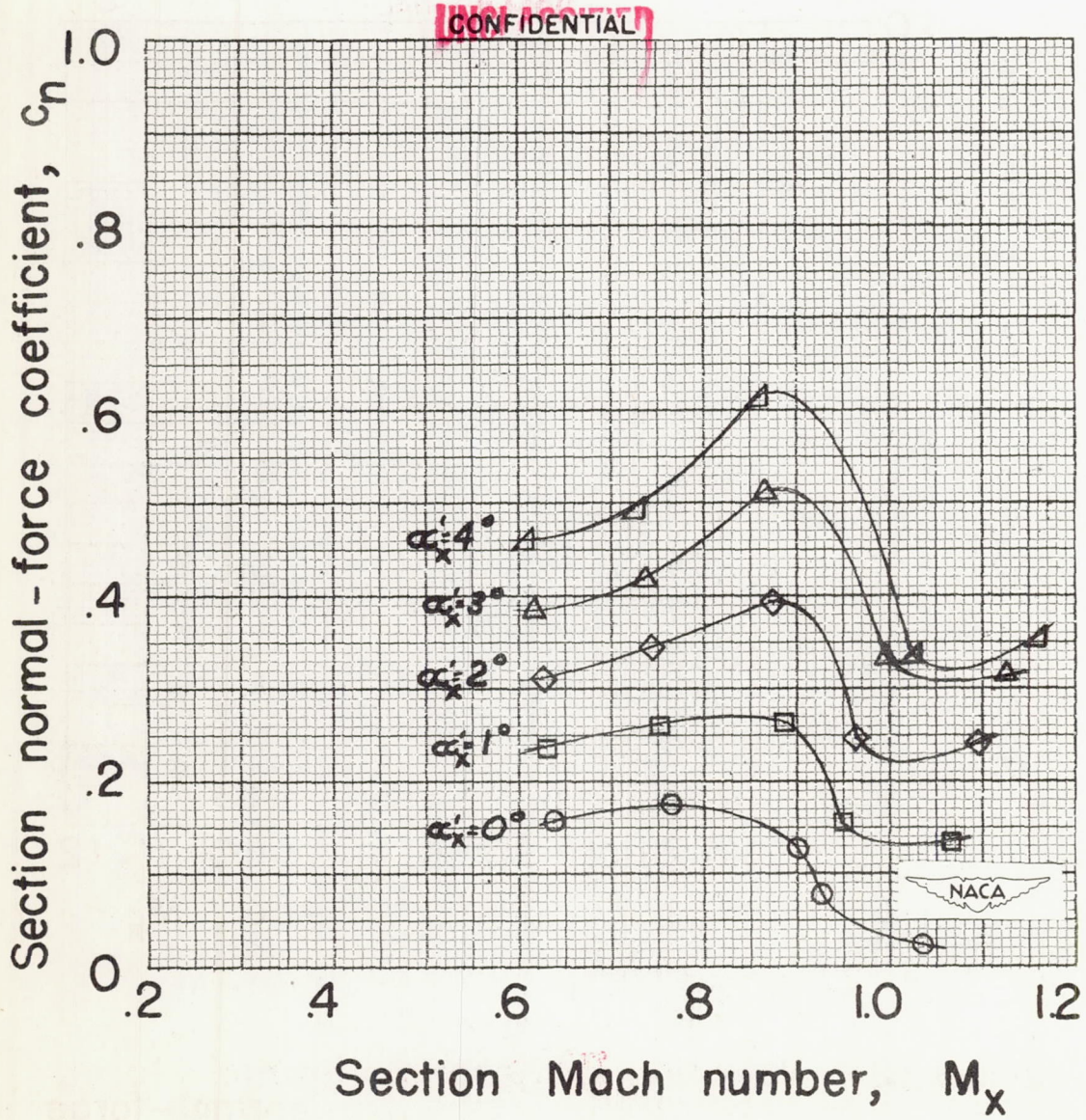


(a) $\beta_{0.75R} = 30°$.

CONFIDENTIAL
UNCLASSIFIED

Figure 12.—Variation of section normal-force coefficient with section Mach number for several angles of attack. Radial station = 0.9.

CONFIDENTIAL

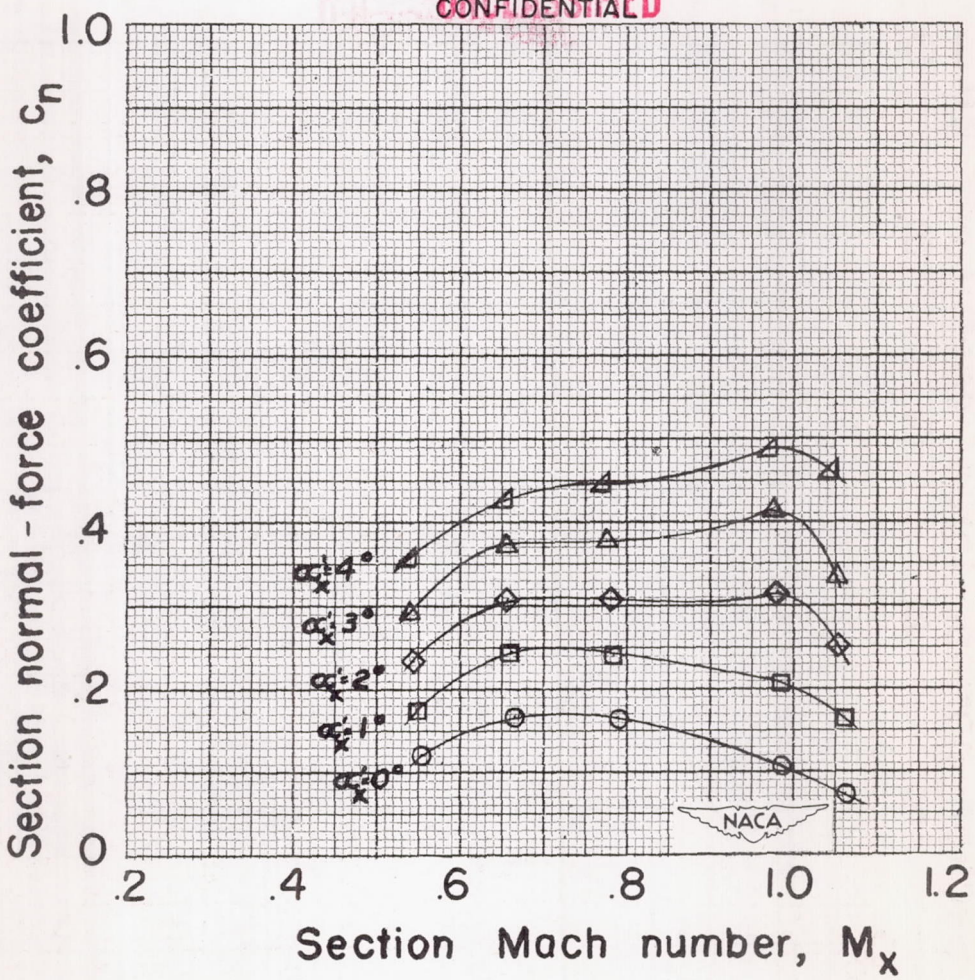


(b) $\beta_{0.75R} = 45°$.

CONFIDENTIAL
UNCLASSIFIED

Figure 12.— Concluded.

UNCLASSIFIED
CONFIDENTIAL

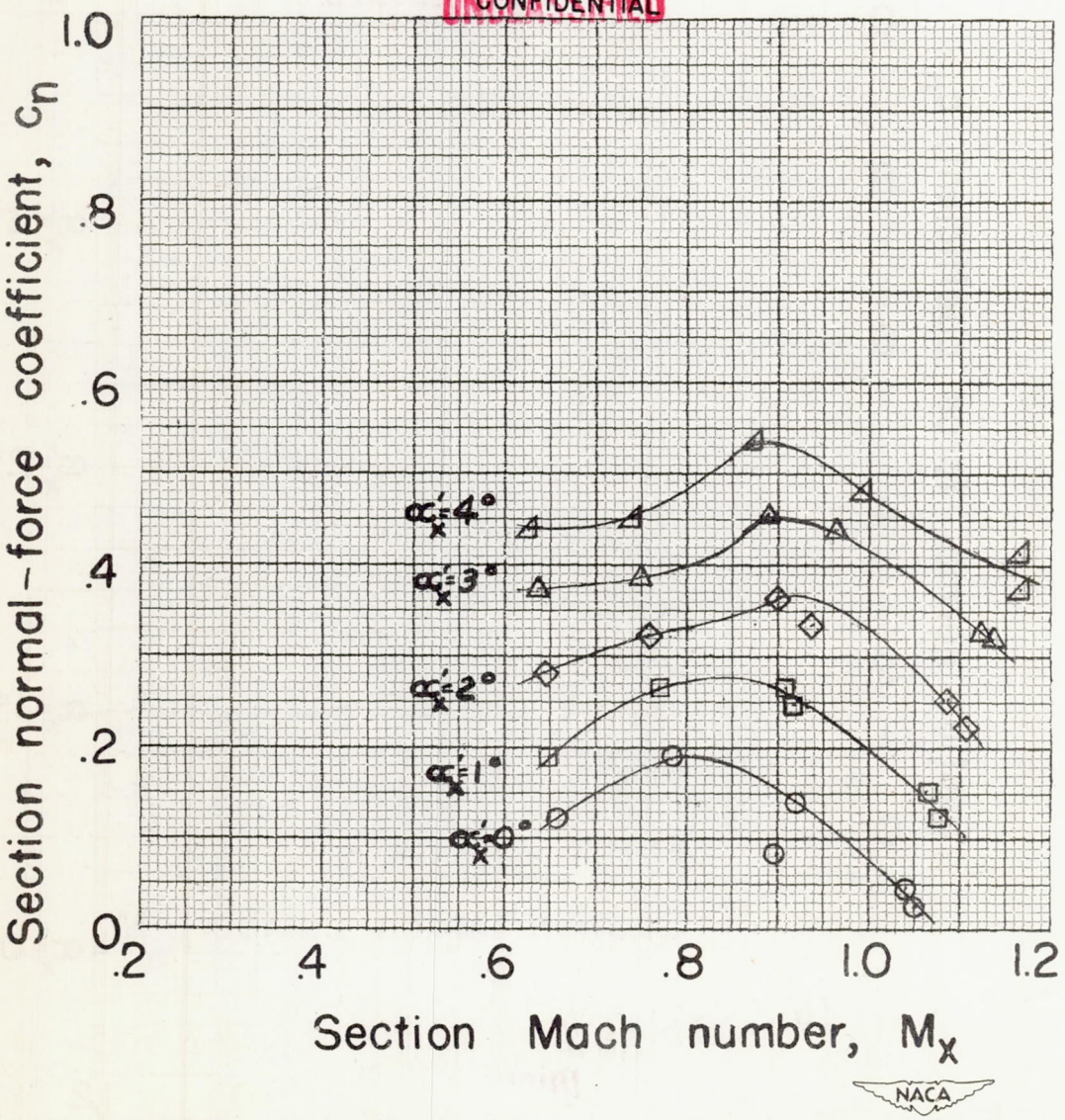


(a) $\beta_{0.75R}=30°$.

CONFIDENTIAL
UNCLASSIFIED

Figure 13.—Variation of section normal-force coefficient with section Mach number for several angles of attack. Radial station=0.95.

UNCLASSIFIED CONFIDENTIAL

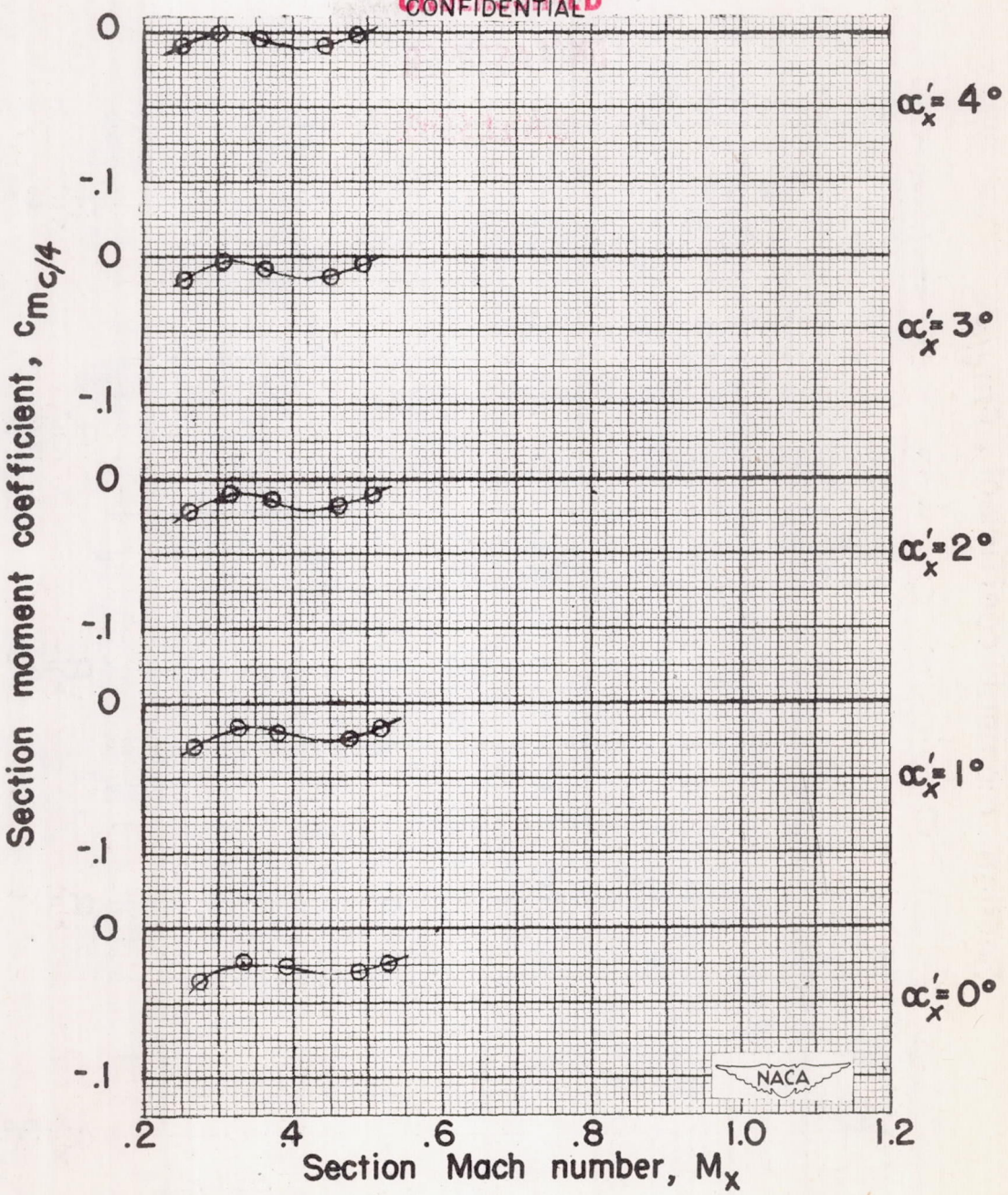


(b) $\beta_{0.75R} = 45°$.

UNCLASSIFIED CONFIDENTIAL

Figure 13.— Concluded.

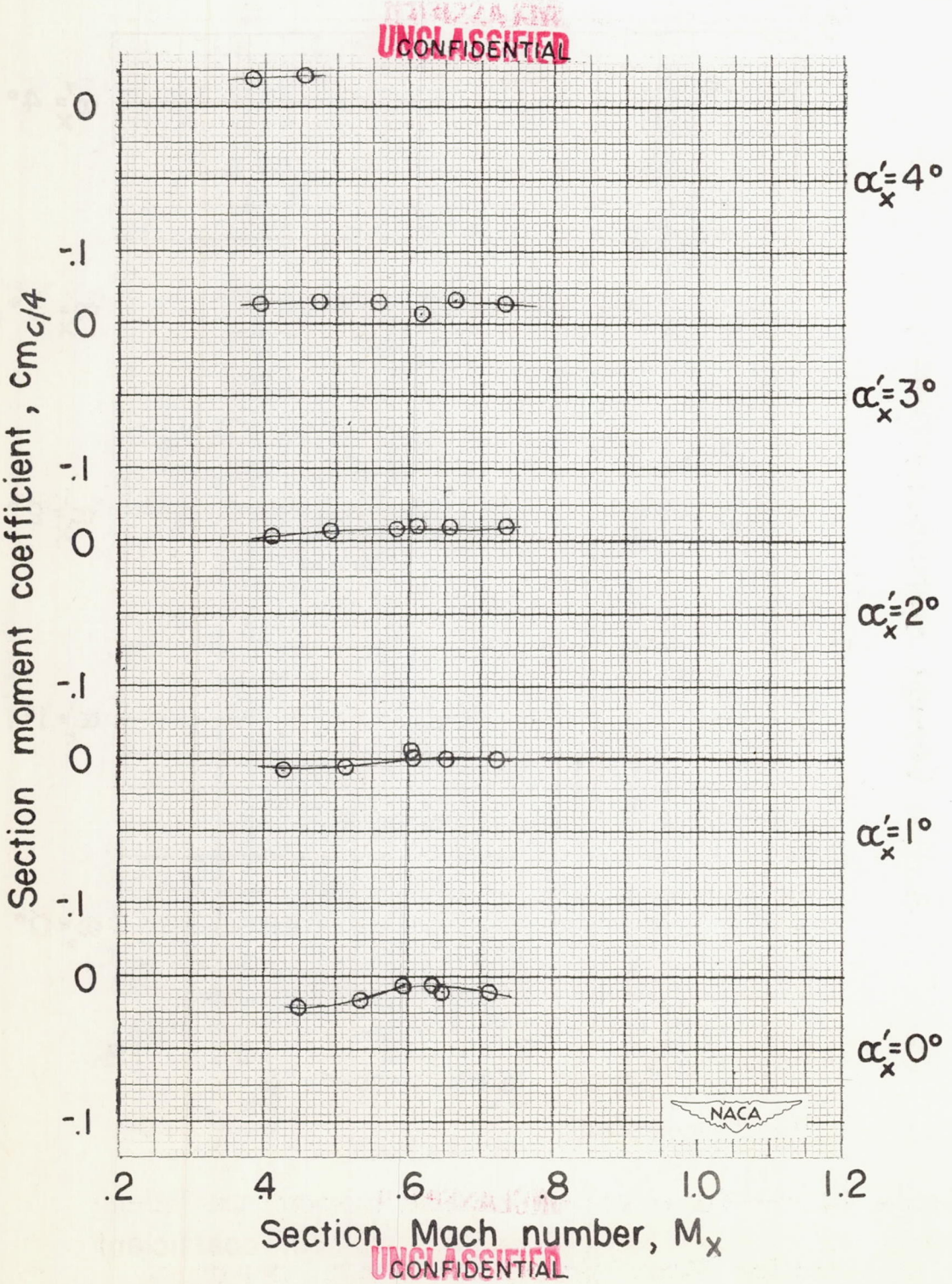
UNCLASSIFIED
CONFIDENTIAL



(a) $\beta_{0.75R} = 30°$.

UNCLASSIFIED
CONFIDENTIAL

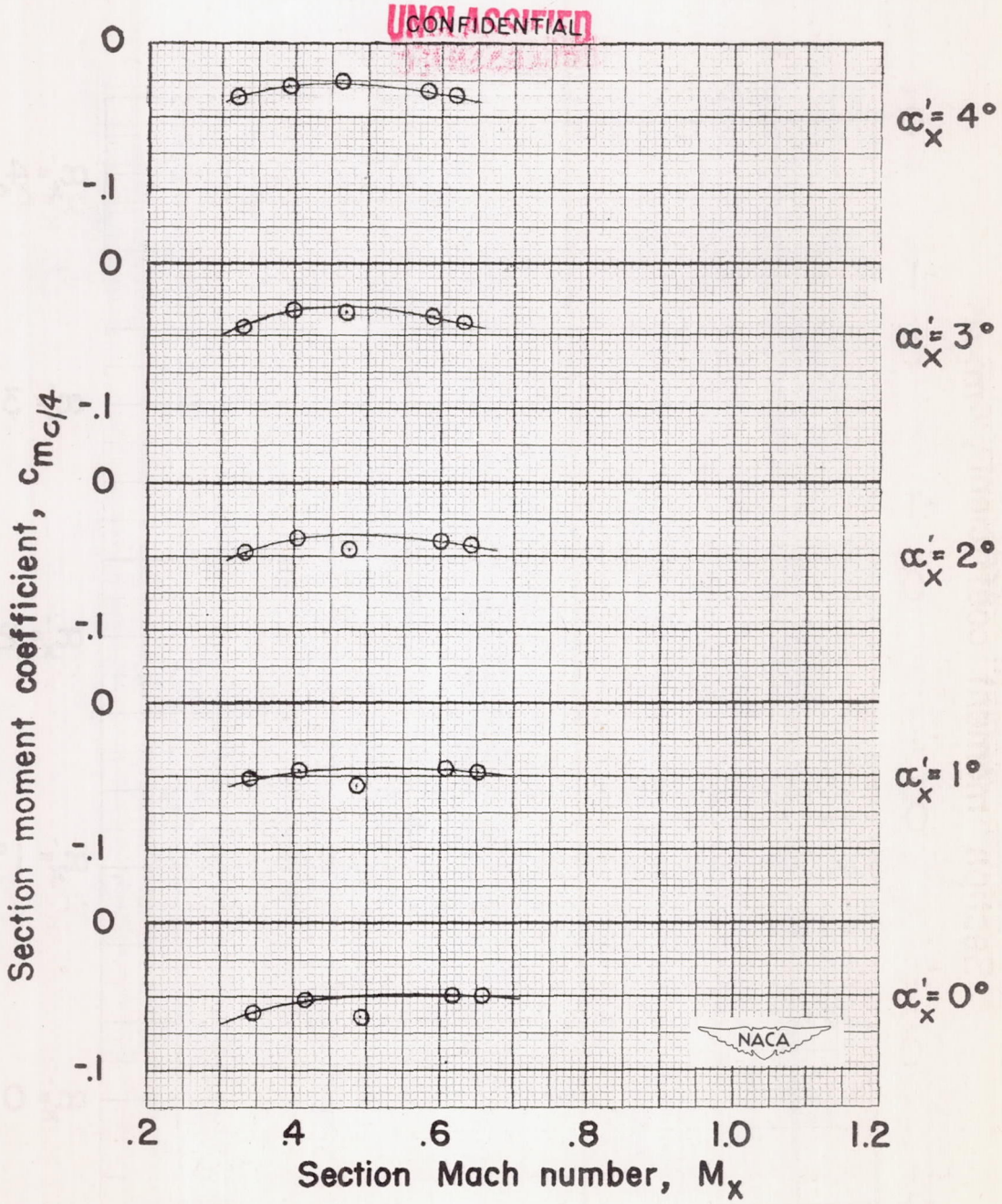
Figure 14.—Variation of section moment coefficient with section Mach number for several angles of attack. Radial station = 0.30.



(b) $\beta_{0.75R} = 45°$.

Figure 14.—Concluded.

UNCLASSIFIED
CONFIDENTIAL

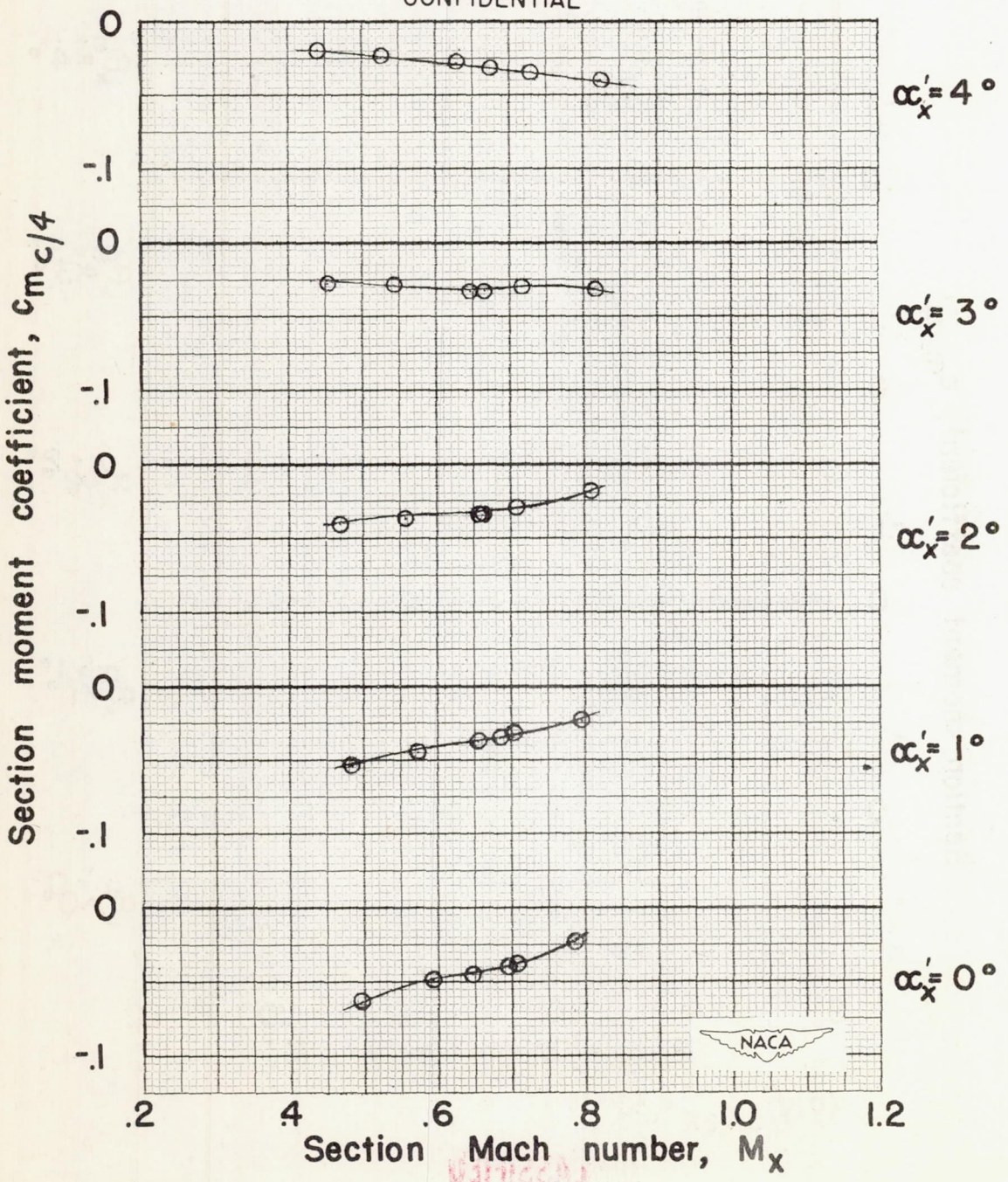


(a) $\beta_{0.75R} = 30°$.

CONFIDENTIAL
UNCLASSIFIED

Figure 15.—Variation of section moment coefficient with section Mach number for several angles of attack. Radial station = 0.45.

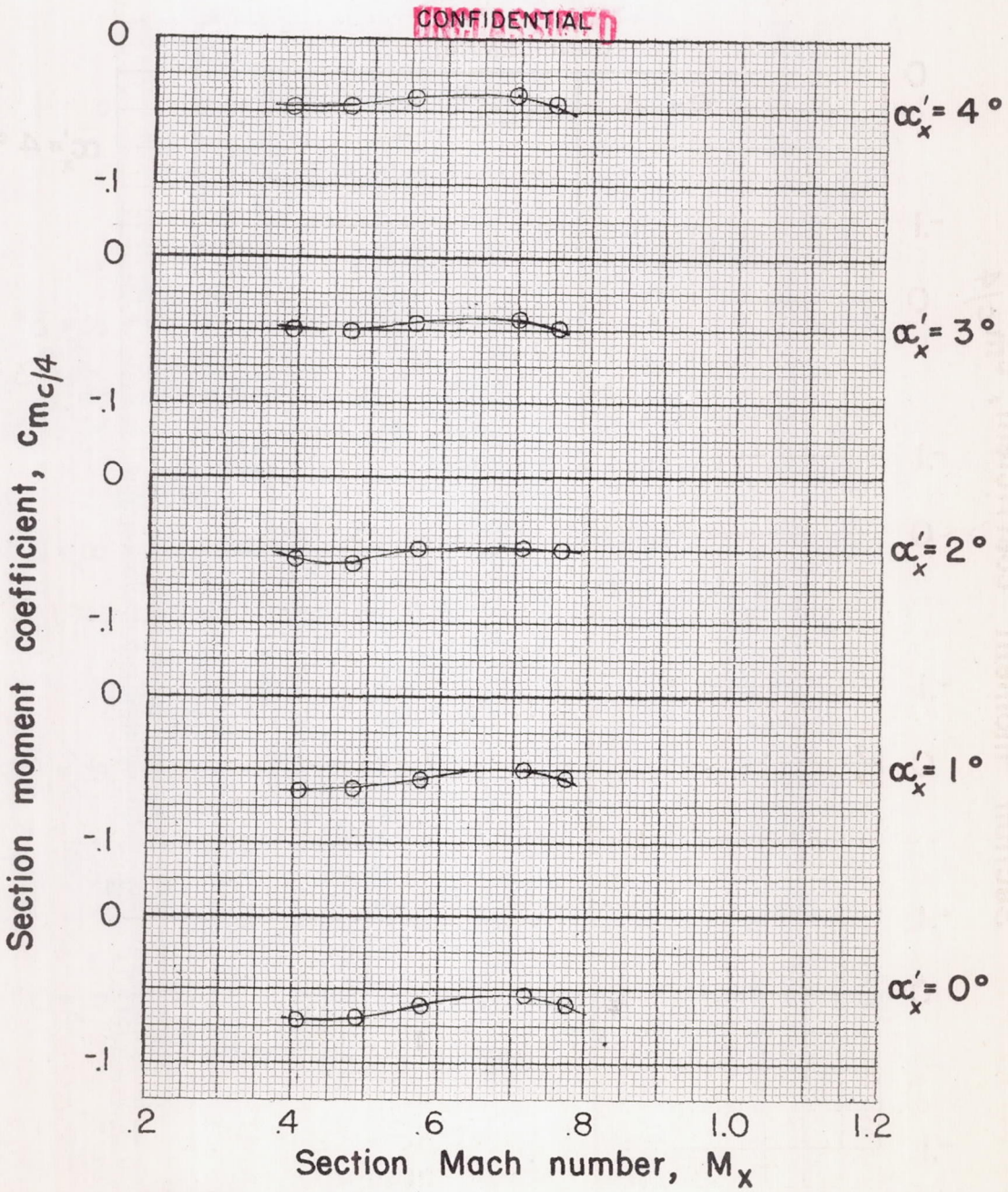
UNCLASSIFIED
CONFIDENTIAL



(b) $\beta_{0.75R} = 45°$.

UNCLASSIFIED
CONFIDENTIAL

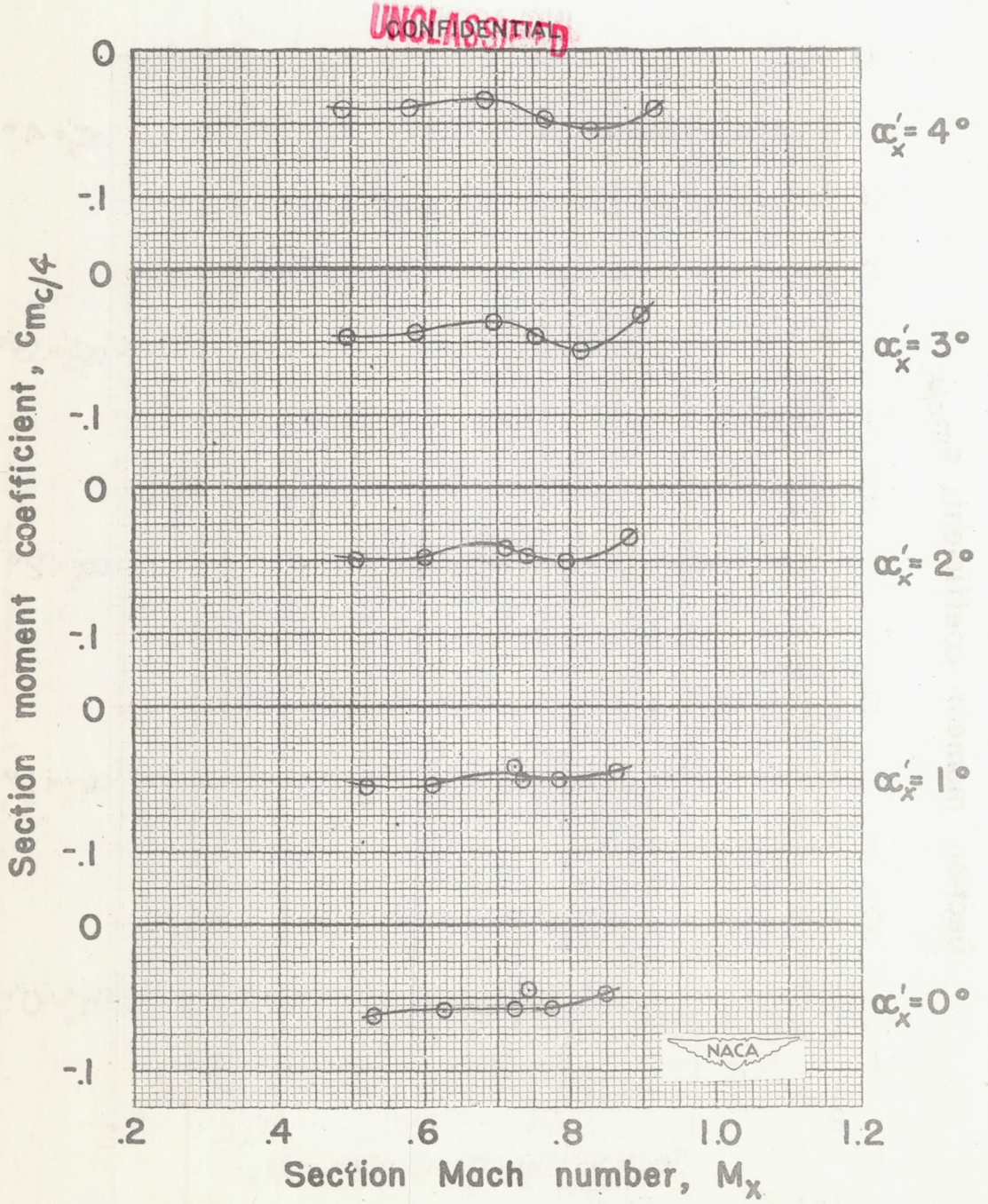
Figure 15.— Concluded.



(a) $\beta_{0.75R} = 30°$.

Figure 16. — Variation of section moment coefficient with section Mach number for several angles of attack. Radial station = 0.60.

UNCLASSIFIED

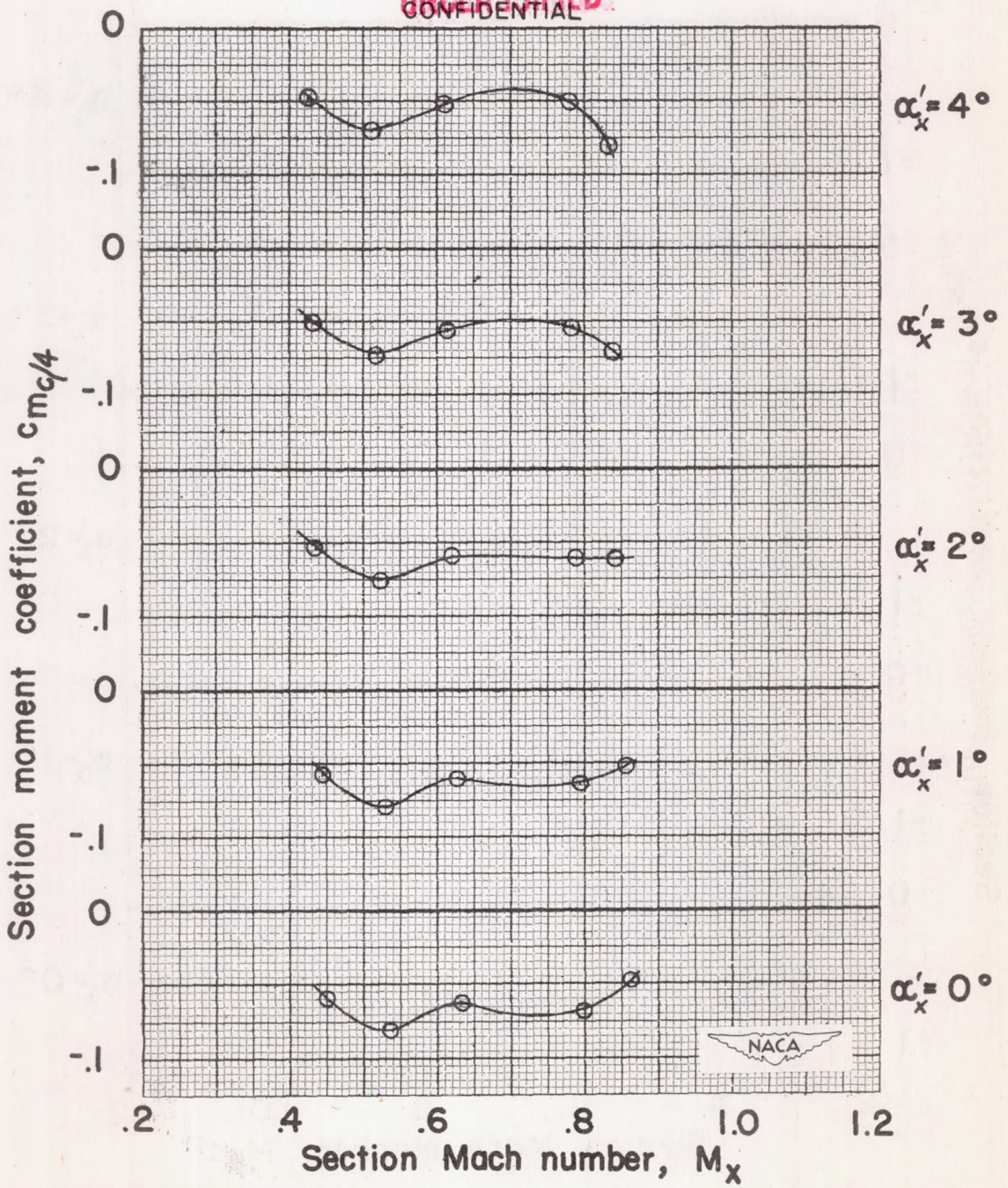


(b) $\beta_{0.75R} = 45°$.

CONFIDENTIAL
UNCLASSIFIED

Figure 16. — Concluded.

UNCLASSIFIED
CONFIDENTIAL

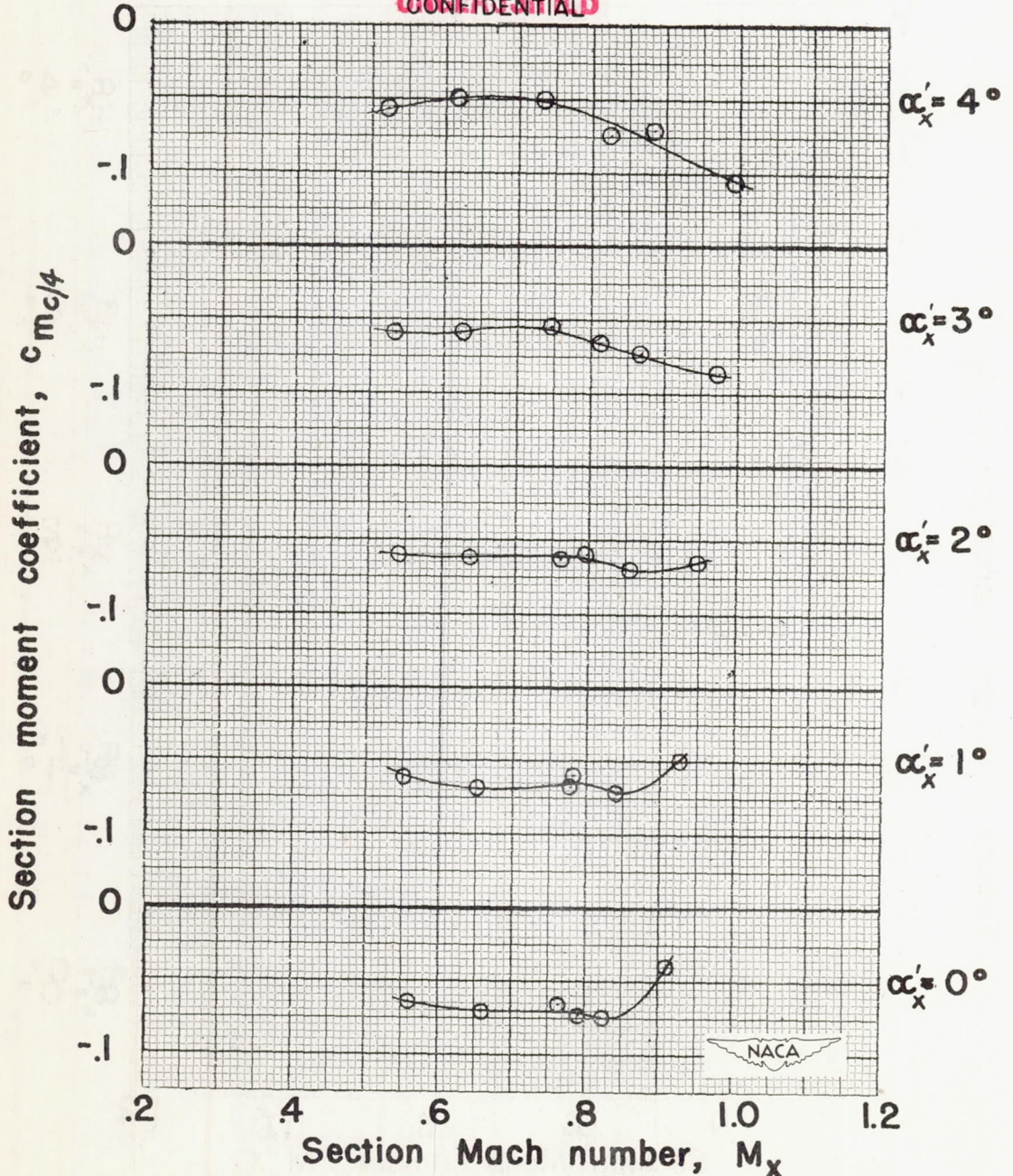


(a) $\beta_{0.75R} = 30°$.

CONFIDENTIAL
UNCLASSIFIED

Figure 17.— Variation of section moment coefficient with section Mach number for several angles of attack. Radial station = 0.70.

UNCLASSIFIED
CONFIDENTIAL

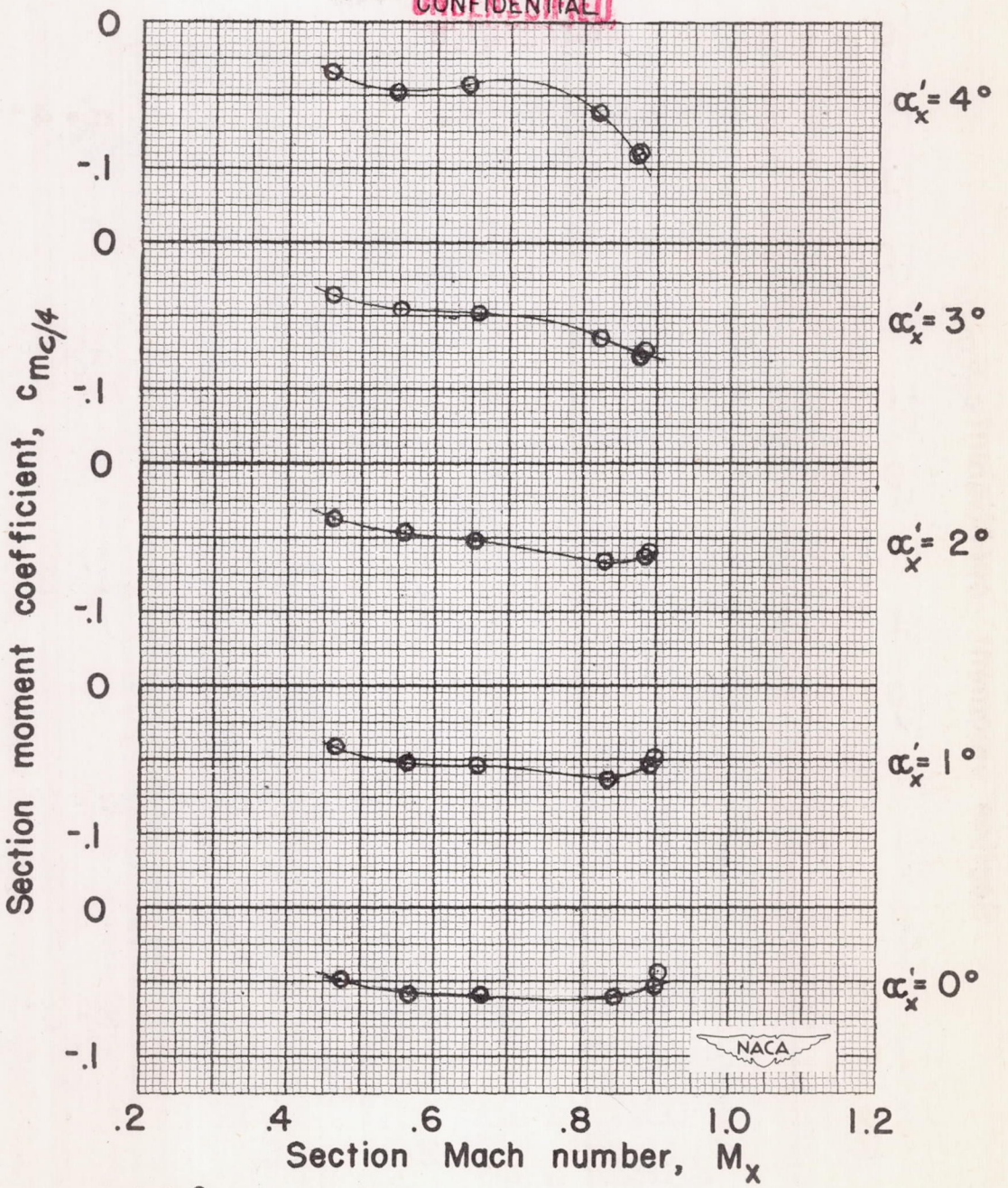


(b) $\beta_{0.75R} = 45°$.

UNCLASSIFIED
CONFIDENTIAL

Figure 17.—Concluded.

UNCLASSIFIED
CONFIDENTIAL

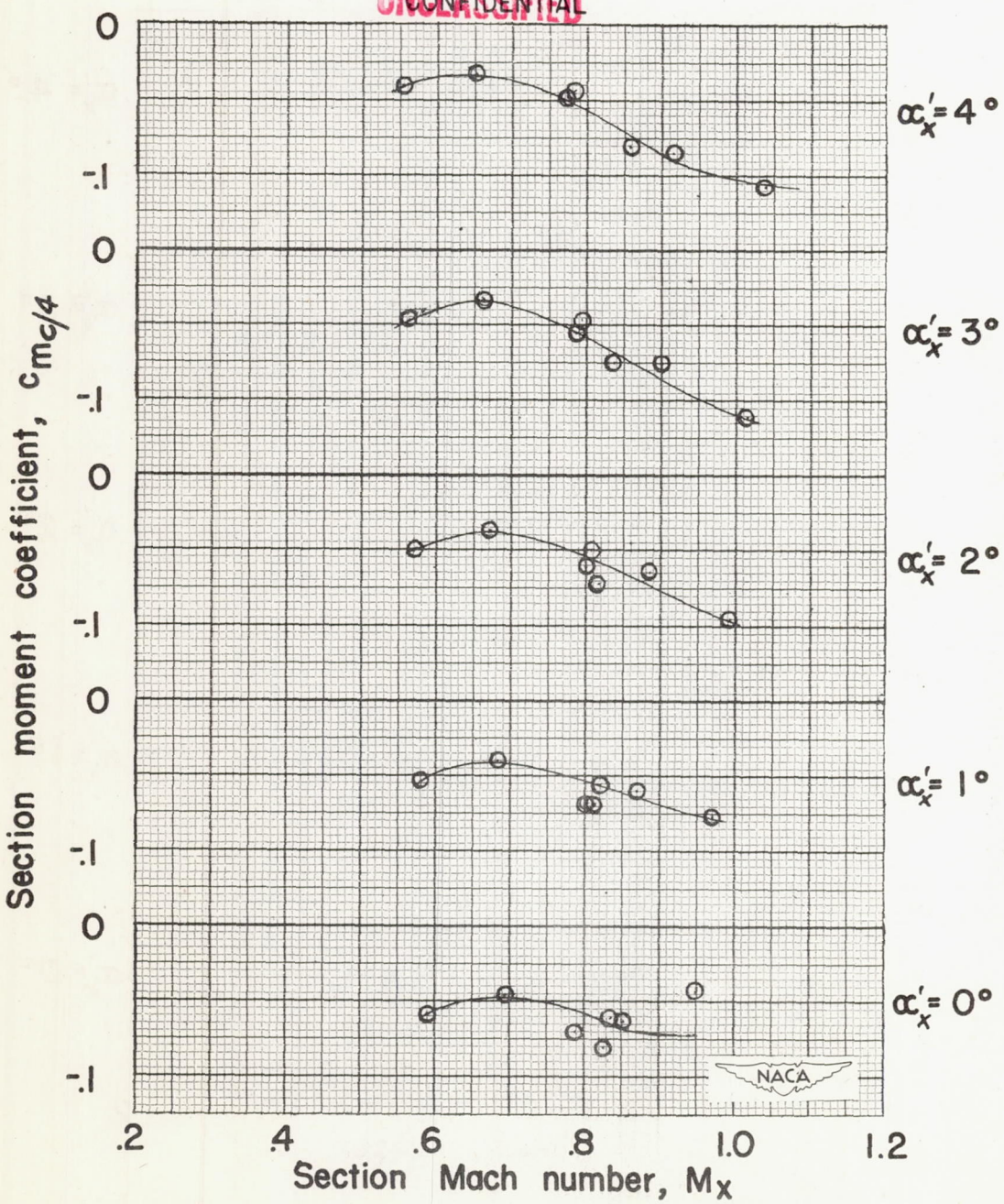


(a) $\beta_{0.75R} = 30°$.

UNCLASSIFIED
CONFIDENTIAL

Figure 18.—Variation of section moment coefficient with section Mach number for several angles of attack. Radial station = 0.75.

UNCLASSIFIED

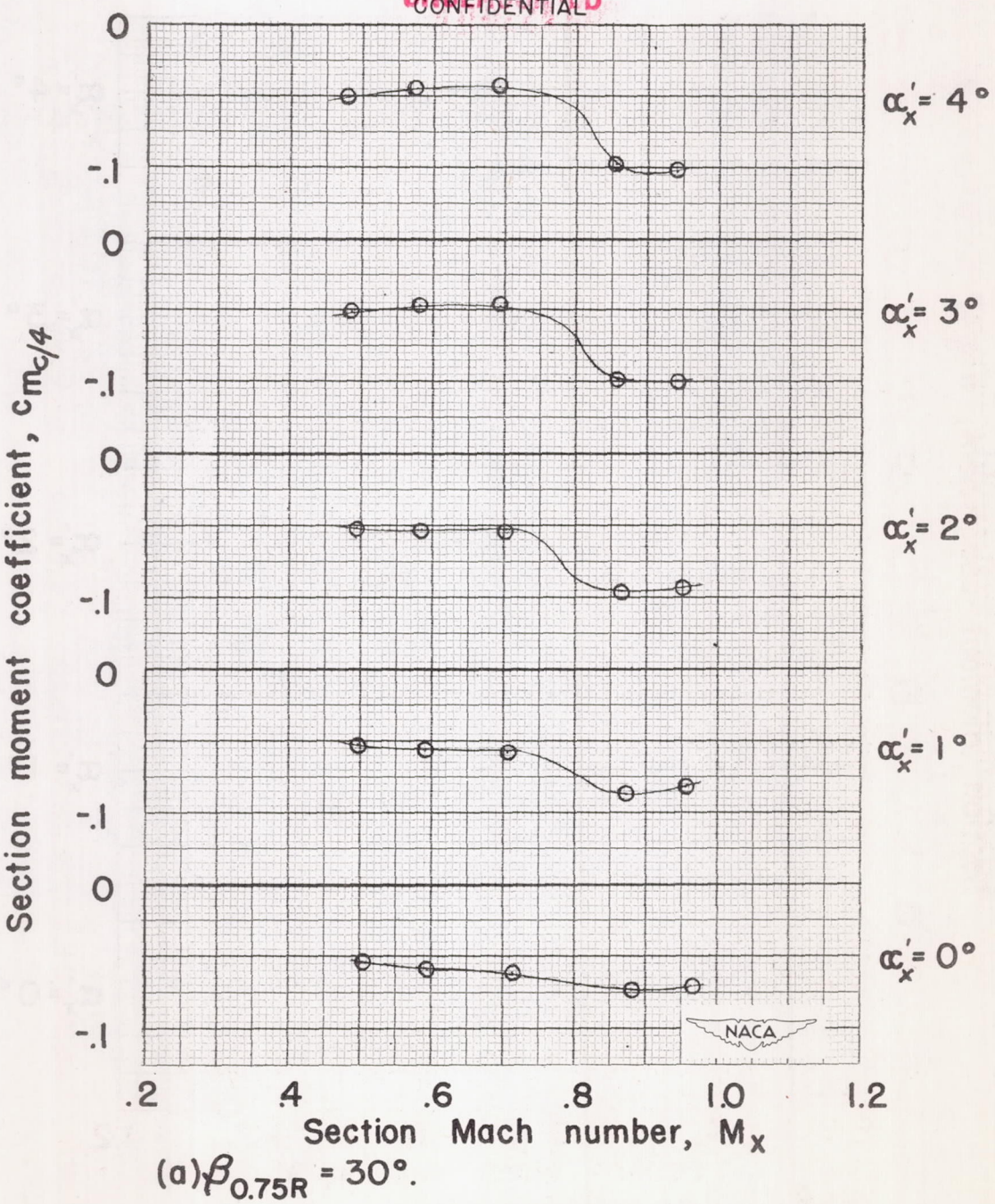


(b) $\beta_{0.75R} = 45°$.

CONFIDENTIAL
UNCLASSIFIED

Figure 18.— Concluded.

UNCLASSIFIED
CONFIDENTIAL

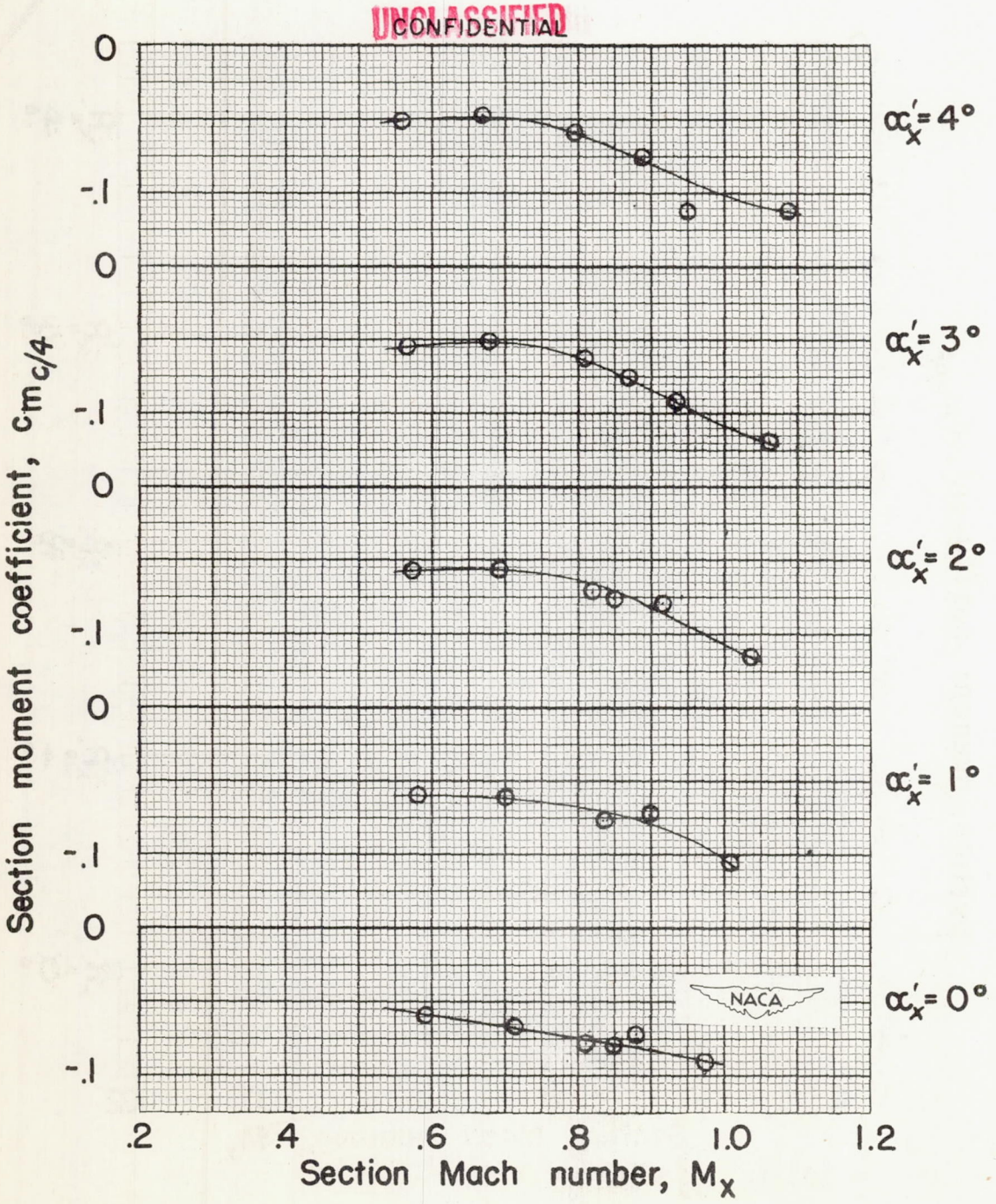


(a) $\beta_{0.75R} = 30°$.

CONFIDENTIAL
UNCLASSIFIED

Figure 19.—Variation of section moment coefficient with section Mach number for several angles of attack. Radial station = 0.80.

UNCLASSIFIED

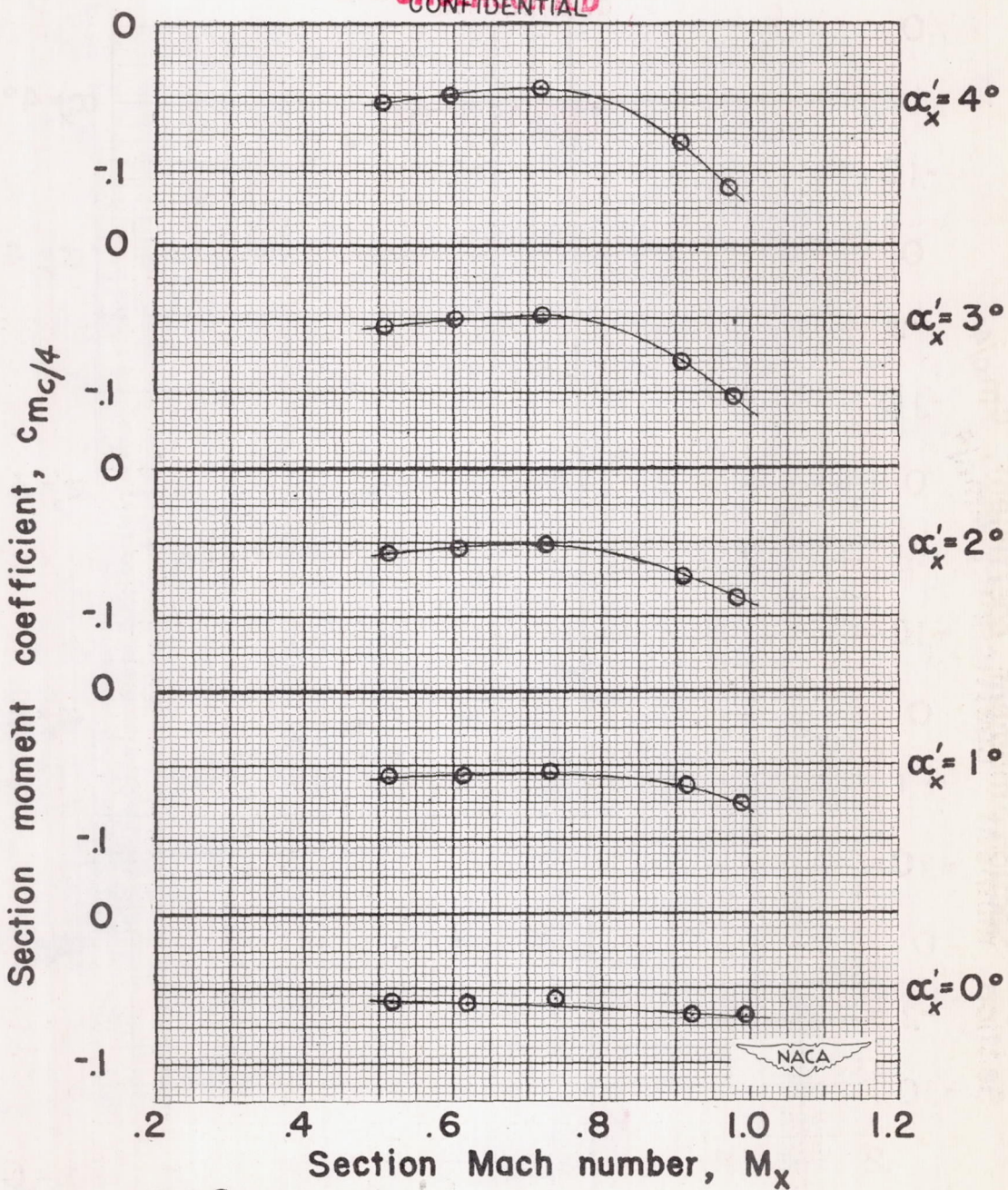


(b) $\beta_{0.75R} = 45°$.

CONFIDENTIAL
UNCLASSIFIED

Figure 19.— Concluded.

UNCLASSIFIED
CONFIDENTIAL

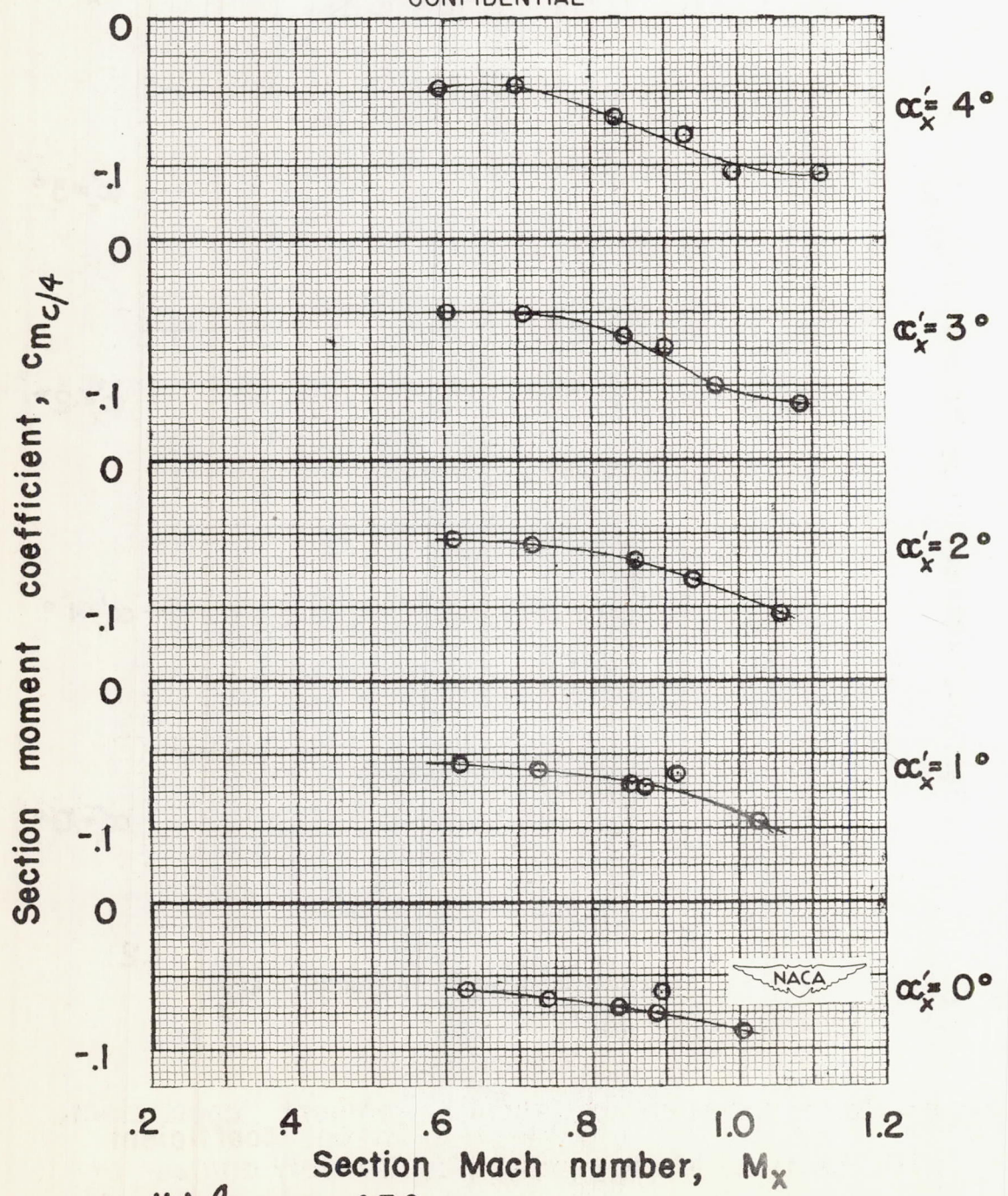


(a) $\beta_{0.75R} = 30°$.

UNCLASSIFIED
CONFIDENTIAL

Figure 20.—Variation of section moment coefficient with section Mach number for several angles of attack. Radial station = 0.85.

UNCLASSIFIED
CONFIDENTIAL

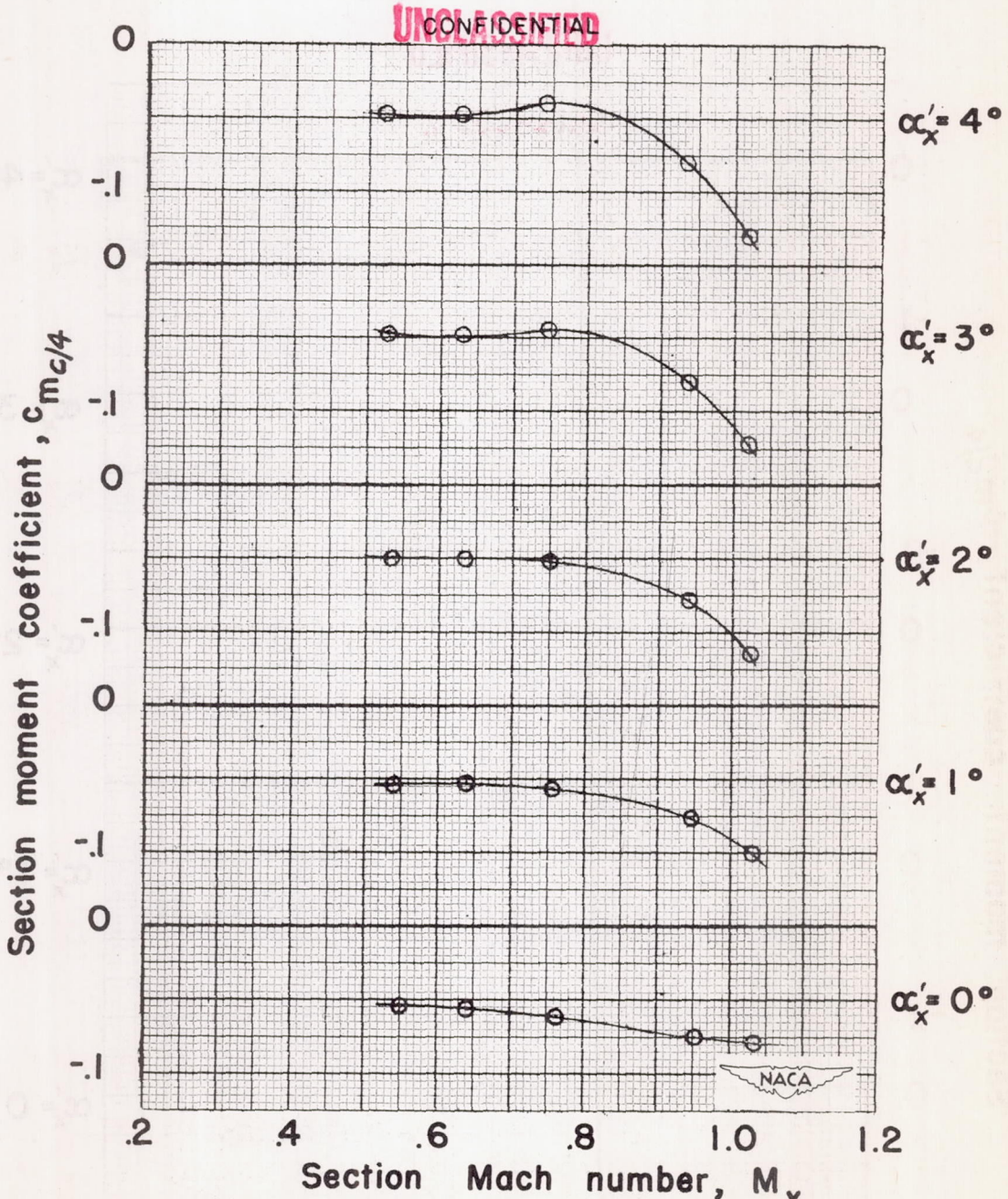


(b) $\beta_{0.75R} = 45°$.

UNCLASSIFIED
CONFIDENTIAL

Figure 20. — Concluded.

UNCLASSIFIED
CONFIDENTIAL

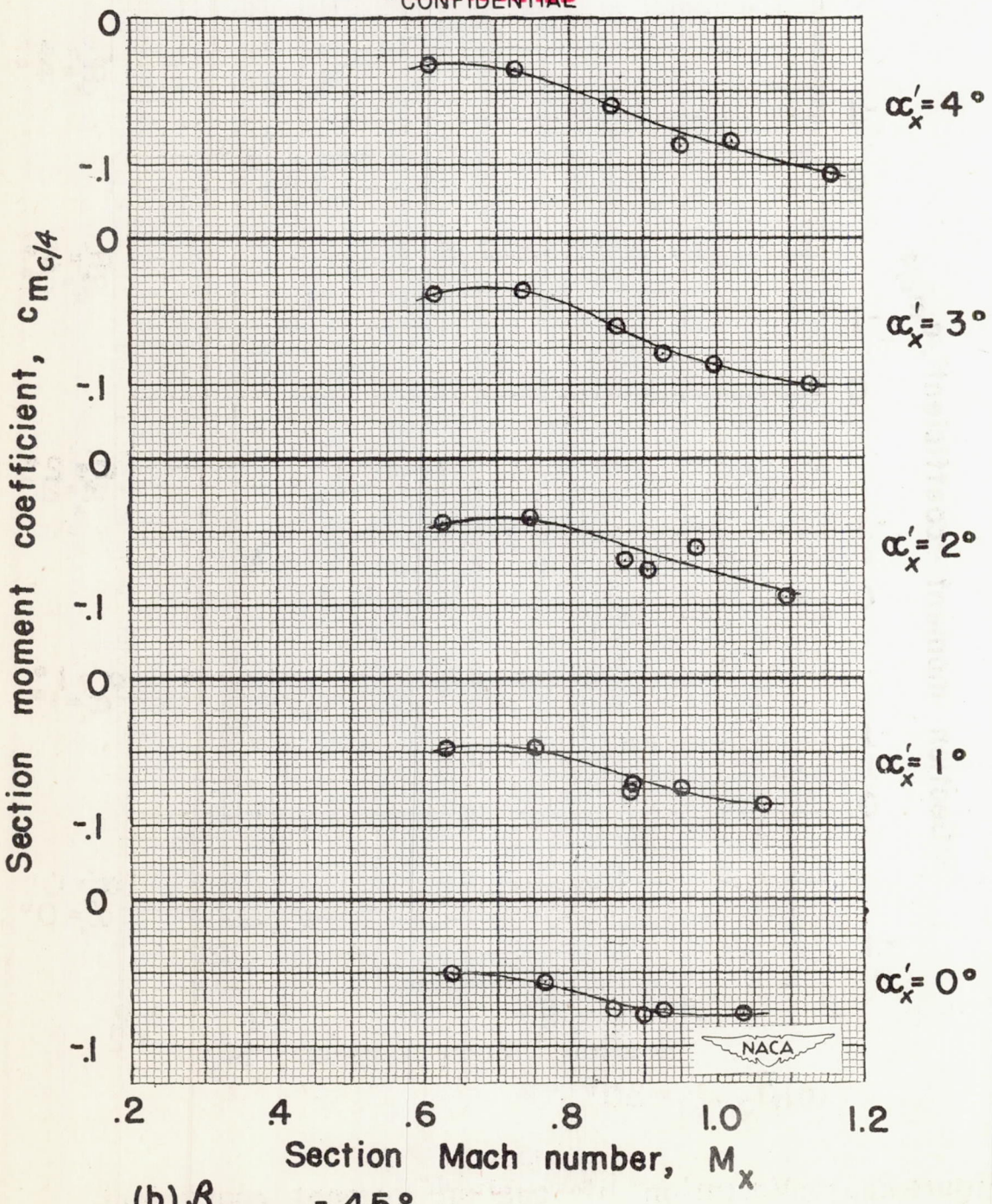


(a) $\beta_{0.75R} = 30°$.

CONFIDENTIAL
UNCLASSIFIED

Figure 21. — Variation of section moment coefficient with section Mach number for several angles of attack. Radial station = 0.90.

UNCLASSIFIED
CONFIDENTIAL

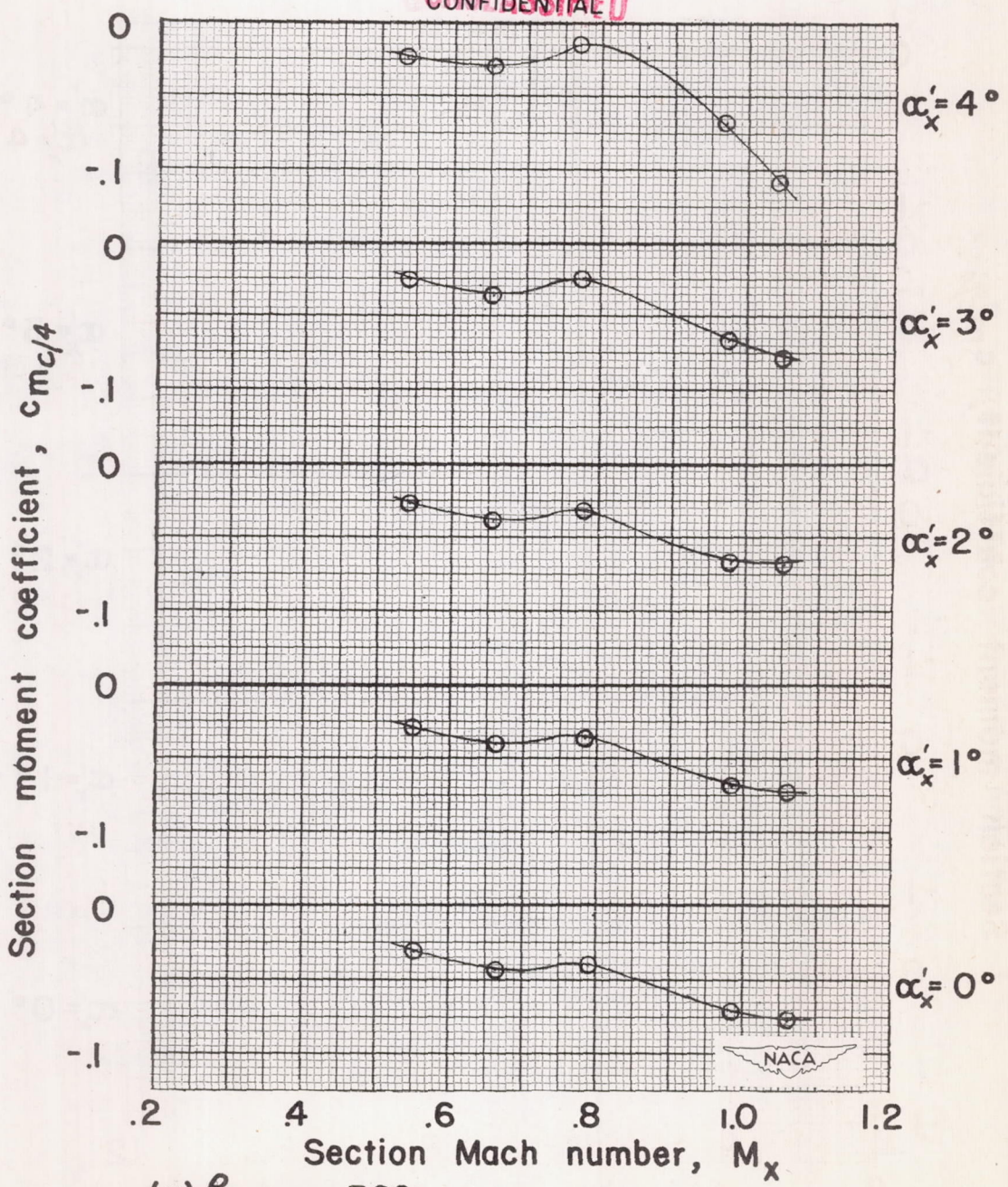


(b) $\beta_{0.75R} = 45°$.

CONFIDENTIAL
UNCLASSIFIED

Figure 21.— Concluded.

UNCLASSIFIED
CONFIDENTIAL

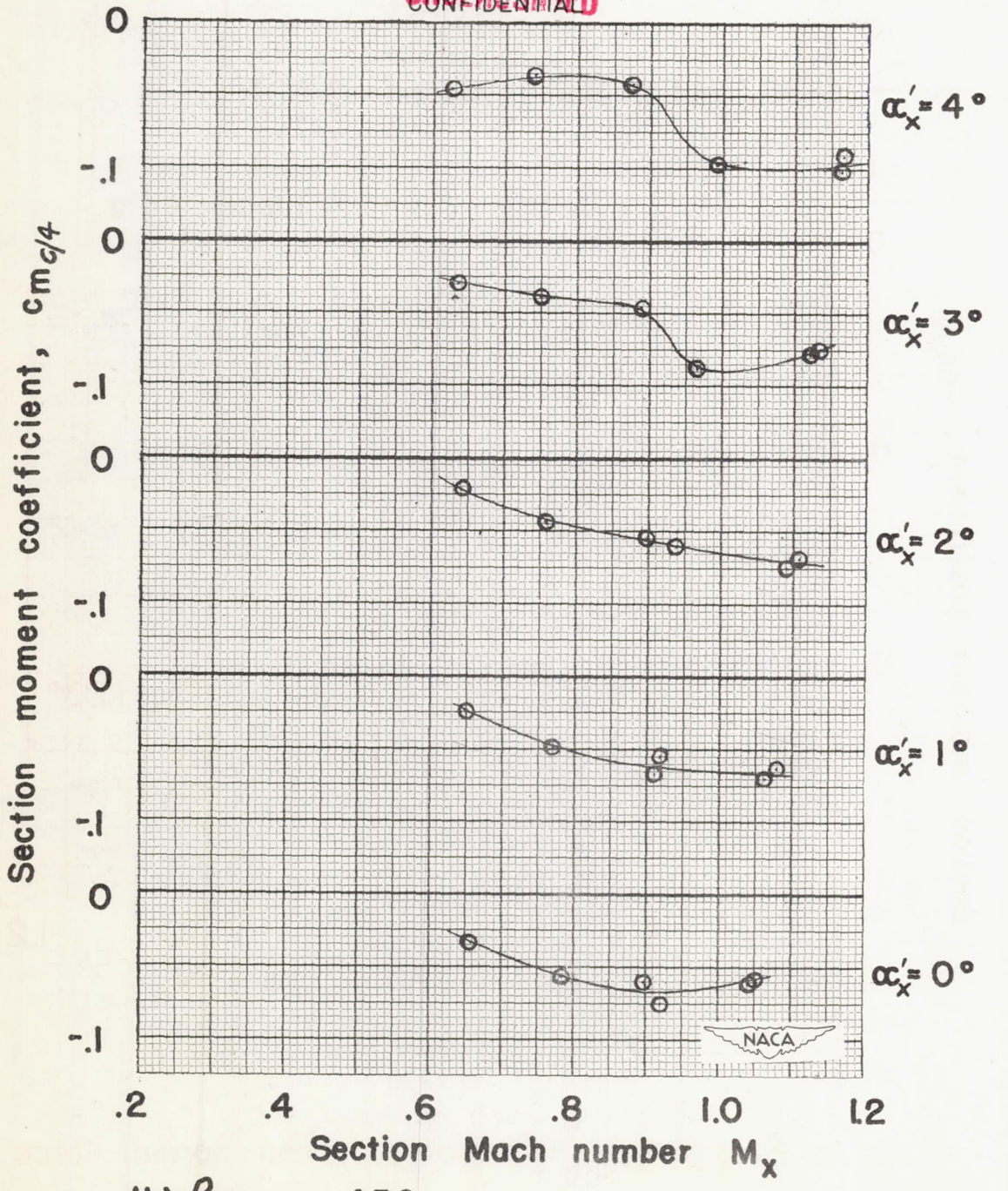


(a) $\beta_{0.75R} = 30°$.

CONFIDENTIAL
UNCLASSIFIED

Figure 22.— Variation of section moment coefficient with section Mach number for several angles of attack. Radial station = 0.95.

UNCLASSIFIED
CONFIDENTIAL



(b) $\beta_{0.75R} = 45°$.

UNCLASSIFIED
CONFIDENTIAL

Figure 22. — Concluded.

UNCLASSIFIED
CONFIDENTIAL

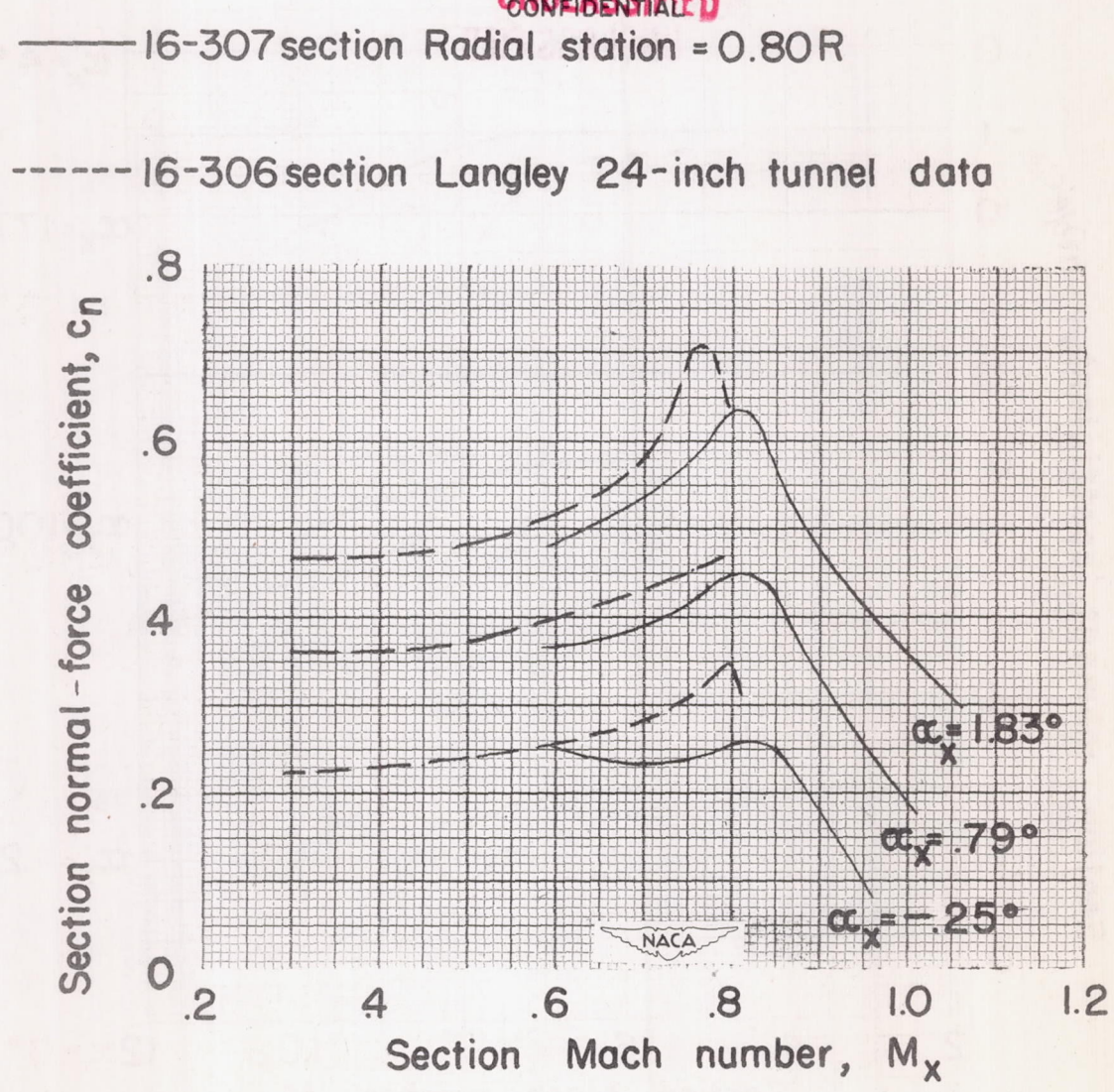


Figure 23.— Comparison of section normal-force coefficient obtained in propeller tests with the lift coefficient obtained in tunnel tests of an infinite aspect ratio model.

CONFIDENTIAL
UNCLASSIFIED

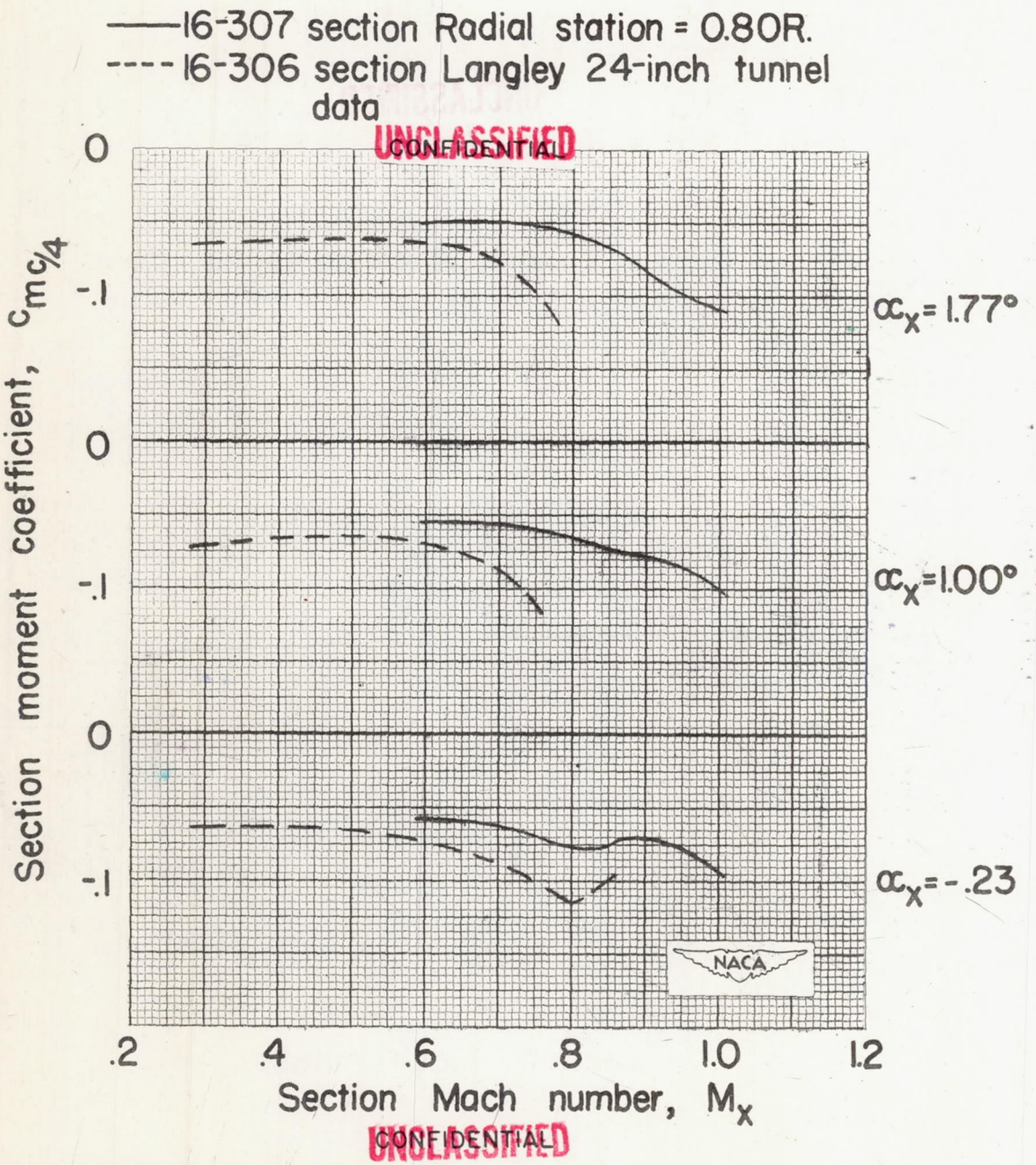


Figure 24.— Comparison of section moment coefficient obtained in propeller tests with the moment coefficient obtained in tunnel tests of an infinite-aspect-ratio model.